Politecnico di Torino

Master's Degree in Energy and Nuclear Engineering
A.Y. 2024/2025
Graduation Session July 2025

Exploring the potential future role of superconducting energy pipelines in the Italian electricity and hydrogen transmission systems

Supervisors:
Laura Savoldi
Matteo Nicoli

Candidate:
Matilde Cais

Abstract

Hydrogen is considered one of the main actors in achieving the decarbonization of the energy sector by 2050. Whilst hydrogen production technologies are already available at an industrial scale, cost-effective solutions for large-scale hydrogen transmission remain limited. In this context, the SuperConducting Energy Pipeline (SCEP) is studied. This technology is capable of simultaneously transporting electricity and liquid hydrogen through a superconducting cable surrounded by an annular pipeline containing liquid hydrogen. Energy System Optimization Models (ESOMs) enable the creation of scenarios to assess the cost-competitiveness of emerging technologies thanks to their detailed techno-economic characterization of energy technologies. This work aims to evaluate the cost-competitiveness of SCEP technology compared to conventional transmission options. The study involves the development of a model instance based on the TEMOA-Italy open-source modeling framework, able to identify the most cost-effective solutions for the investigated future scenarios. The model developed for this study focuses on the Italian power and hydrogen sectors and features regional resolution. Several scenarios concerning emission reduction targets, hydrogen generation from biomass, and involving different assumptions for the techno-economic performance of SCEP are investigated to identify the conditions determining the cost-effectiveness of the technology. The variation in the installed capacity of SCEP technology between adjacent regions is assessed by varying both its investment cost and the costs of traditional electricity transmission, simulating an increase in aluminium and copper cost. SCEP becomes a cost-effective solution when assuming 70% reduction in its future investment cost, and 40% if assuming a double cost for traditional lines with respect to the historical values. The installation of SCEP encourages hydrogen generation centralized in regions with higher renewable capacities. The model created is a useful tool to consider regional specificities while representing the Italian power system. SCEP technology appears as a potential solution that may contribute to Italy's decarbonization objectives, although its deployment would depend on specific cost and policy conditions.

List of acronyms

AEM	Anion Exchange Membrane
CCS	Carbon Capture and Storage
CCUS	Carbon Capture, Utilization and Storage
CF	Capacity Factor
CHP	Combined Heat and Power
ESOM	Energy System Optimization Model
GDP	Gross Domestic Product
GHG	Greenhouse Gas
INECP	Integrated National Energy and Climate Plan
LH_2	Liquid Hydrogen
NUTS	Nomenclature of Territorial Units for Statistics
O&M	Operation and Maintenance
PEM	Proton Exchange Membrane
PSOM	Power System Operational Model
SCEP	SuperConducting Energy Pipeline
SDD	Scenario Description Document
SOEC	Solid Oxide Electrolysis Cell
TEMOA	Tools for Energy Modeling Optimization and Analysis
TSO	Transmission System Operator

List of tables

List of figures

Table of Contents

Chapter 1

Introduction

1.1 Evolution of transmission systems in the energy transition context

The expansion and modernization of transmission grids is set to become essential for the energy transition [1]. As the energy system electrification is increasing to facilitate decarbonization, the importance of power transmission has grown [2]. An efficient transmission grid increases the cost effectiveness of renewable capacity installations for regions where the spatial distribution of renewable generation potentials does not match the demand distribution [3]. Transmission grids need to be modernized and expanded through a comprehensive approach considering both the economical and technical aspects of grid operation, and the policy framework the grid operates in [4].

The transmission of electric power via cables is the standard option to link electricity production and consumption. Due to its favourable mechanical properties and low costs, the most used conductor type is aluminium conductor steel reinforced, while aluminium alloys and copper are usually adopted where the mechanical stresses are lighter and the priority is on increasing the cable conductibility [5]. As transmission distances and the transmitted power increase, minimizing transmission losses becomes crucial. In this context, research has increasingly focused on superconductors, which allow electricity transmission with negligible power losses [6]. However, for superconductors to become a practical substitute for part of the existing transmission infrastructure, significant cost barriers must be addressed, along with the integration of efficient cable cooling systems [7].

Within the European context, both the REPowerEU Strategy [8] and the European Strategy for Hydrogen [9] identify hydrogen as a vector to facilitate the decarbonization of hard-to-abate sectors – such as transport and industry – while enhancing energy security. Additionally, hydrogen is recognized as a potential electricity storage option, complementing batteries and fuel cells [9]. Increasing the energy system reliance on hydrogen will require to develop an efficient hydrogen transport network, both at European and national level [9]. Although technologies for hydrogen transport are available, their cost limits their application to point-to-point delivery, from the production site to the location where the demand occurs. However, growing the need for long-distance energy transmission, hydrogen could become the energy carrier employed as a viable alternative to conventional electricity transmission [10], [11].

1.2 Hybrid cables and the SuperConducting Energy Pipeline

In this framework, the concept of hybrid cables is developed. Past studies [12], [13] have explored the use of cryogenic fuel, e.g. liquid hydrogen, as a cooling medium for superconducting cables [14], enabling the simultaneous transmission of electrical energy, chemical energy and cooling potential to improve the overall efficiency of energy transmission. Serving multiple functions at once could help overcome the high installation costs of the technology, making it more appealing despite its upfront economic challenges [15]. Recently, various studies investigated the use of hybrid cables as energy transmission means for transport applications (specifically for railway transportation [15]) to connect renewable energy sources – either onshore or from offshore installations – with ports, ground transport and industries in need of both electricity and hydrogen [16], [17].

In the context of hybrid cables, one of the technologies being studied is the SuperConducting Energy Pipeline (SCEP), enabling the simultaneous transfer of electricity and liquid hydrogen (LH_2). The SCEP is composed of a superconducting cable in MgB_2 (magnesium diboride) allowing the transfer of electric power, while liquid hydrogen is the cryogen that cools the cable and transfers chemical power [17]. The study of the design of such technology is not a novelty in literature [18]: various design

configurations have been studied, particularly concerning transmitted powers around 1 GW_e or larger [16], [19]. In 2024, an innovative design for a SCEP configuration with a nominal power of 300 MW_e has been proposed, while the design of the active auxiliaries, the thermo-mechanical evaluation and the analysis of the pipeline operation in fault conditions are currently being assessed [17]. As SCEP remains in the early stages of development, significant uncertainties remain regarding its techno-economic parameters, particularly with respect to large-scale deployment. For this reason, an economic evaluation of SCEP technology should be coupled with a sensitivity analysis to evaluate the maximum cost of the technology making its installation profitable.

The study of SCEP technology is one of the Research Projects of Significant National Interest (RPNI) [17] in the framework of the Italian National Hydrogen Strategy [20]. The cited technical and economic feasibility study of SCEP aims to investigate the use of the technology to connect the offshore energy hub in the proximity of Ravenna port [21], part of the Adriatic Green Network of Energy Sources (AGNES) project [22]. The AGNES project energy hubs 1 and 2 are currently undergoing the authorization process as from [22] but the connection to the grid on the mainland has already received the approval from the Italian Transmission System Operator (TSO) Terna [23]. For this reason, SCEP is not proposed here as a connection alternative for AGNES energy hubs 1 and 2, but the purpose is to investigate whether the technology could be a possible solution for similar projects, comparing its performance and cost to the ones of traditional transmission technologies.

In summary, although the concept and preliminary designs of the SuperConducting Energy Pipeline (SCEP) have been proposed, a significant research gap remains in the techno-economic literature assessing its competitiveness as a transmission option, particularly under different cost assumptions and deployment scenarios.

1.3 Modeling tools for the energy transition

Energy models are powerful tools as they represent complex system used to execute exhaustive scenario analyses. They aim to represent phenomena or conditions which cannot be described or captured through experiments, as impracticable or too costly [24]. Two different approaches can be employed when modeling transmission systems at multi-regional level: Energy System Optimization Models (ESOMs) or Power System Operational Models (PSOMs). Due to their different nature, the former provides a better description of capacity expansion with longer time scales, while the latter allow to observe the operation of the electric grid and to its interaction with power generation and consumption systems and storage [25].

ESOMs aim to find optimal solutions – often in terms of cost – for energy systems under defined constraints [26]. They are often used for short-term dispatch planning and to explore different scenarios to evaluate long-term investment planning [27]. Constraints in ESOMs usually aspire to represent technical and physical restrictions, or to model socioeconomic and environmental limitations, such as on greenhouse gas emissions [27].

Among ESOMs, different modeling frameworks have been developed. This includes the bottom-up tool TEMOA (Tools for Energy Modeling Optimization and Analysis), which presents:

a. Technology-explicitness: each technology is characterized by its technical and economic parameters.
b. Possibility to represent the energy system under investigation as a network of more spatial regions.
c. Partial equilibrium in competitive markets with perfect foresight.

The model operates with a linear programming algorithm, and its objective function is the minimization of the total cost of the energy system during the model time horizon [28].

Despite the recognized crucial role of transmission systems in achieving decarbonization targets, a significant knowledge gap remains in this field. Tools capable of comprehensively representing the techno-economic competition between traditional and innovative transmission technologies (e.g., the SCEP) within the energy system are currently lacking.

1.4 Aim of the thesis

The aim of the thesis is to study the potential role of the SCEP in the Italian energy system. Due to the distribution of resources and energy demand, Italy provides an ideal case study for assessing the techno-economic viability of this technology. In fact, despite its relatively small extension, Italy is characterized by strong regional differences both regarding its socio-economical features [29] and resources distribution [29], [30]. These aspects affect the energy intensity of each region and the capacity factors of various generation technologies – defined as the ratio of the output of a generation plant over a period of time, to its potential nominal output if operating constantly at full nameplate capacity over the same period of time [31]. As a result, a mismatch between areas with high electricity demand and others with high resource availability occurs, making interregional transmission a crucial element of the Integrated National Energy and Climate Plan (INECP) [32], in accordance with Terna Scenario Description Document (SDD) of 2024 [33]. As the decarbonization of the power sector accelerates and the integration of variable renewable energy sources increases, an increased connectivity is essential for efficiently balancing supply and demand across the country [34], [35].

When focusing on transmission in energy systems, interconnection is a key aspect to be considered. Indeed, it is necessary to use instruments capable of characterizing the interaction between two or more regions able to exchange energy commodities. A mathematical model of the power sector of each Italian region overcomes the limitations of considering the country as a single node neglecting its intrinsic regional differences [36]. At the same time, the electricity transmission network can be modeled and compared to new alternatives for energy transmission technologies [37].

To carry out this analysis, a multi-regional model of the Italian power and hydrogen sectors is developed. The model is based on TEMOA-Italy, a model instance for the optimization of the Italian energy system developed by MATHEP Group at Politecnico di Torino within an extended version of the TEMOA modeling framework [28]. Using ESOMs – and in this case TEMOA model – allows the quantification of the cost thresholds for SCEP to play a meaningful role in the national energy system as a competitive alternative to conventional transmission technologies. To address the uncertainty inherent in SCEP's cost estimates, a sensitivity analysis is performed.

In Chapter 2 are presented the modeling framework, including the structure of the power and hydrogen sectors of the multi-regional model, the input data required for the characterization of the technologies and the main model constraints. Then, the explored scenarios are discussed along with the hypotheses introduced for their formulation. Lastly, the assumptions for the sensitivity analysis to verify SCEP cost efficiency are presented. Chapter 3 includes the discussion of the explored scenarios, the results for the electricity and hydrogen sectors, and the investigation of the cost barrier for SCEP to become a viable transmission option in the Italian energy system.

Chapter 2

Methodology

2.1 Model structure

As introduced in the previous Sections, a multi-regional model for the Italian power and hydrogen sector is developed. The model structure follows the TEMOA-Italy characterization of power sector and hydrogen sector, where both are part of the supply-side of the energy system [28].

The model covers the period from 2022 to 2050. Specifically, 2022 serves as the base year, representing the first time-period of the model in which the energy system is fully characterized. The base year is the starting point for building the model: national and regional energy balances [38] are analysed to define regional service demands and the technology mix required to meet them. Moreover, the techno-economic characteristics of each technology in the mix are known. The model is then optimized from 2025 on, with a time-step of five years, specifically including 2025, 2030, 2035, 2040, 2045 and 2050. For each milestone year, the optimal technology mix for each region is calculated by minimizing the cost of the system while satisfying the electricity and hydrogen demands.

The model adopts a simplified time resolution by dividing the year into four seasons, each representing one quarter of the year. Within each season, a representative day is modeled using 24 hourly time slices, resulting in a total of 96 time slices per year. Even though the modeling framework chosen does not allow a close representation of the intermittency inherent in renewable electricity production [39], this time-resolution is selected to represent accurately the seasonal and daily fluctuations in the output of renewable technologies using average representative days. In fact, being the focus on the power sector dynamics, it is crucial to have an accurate time-resolution to represent both power and energy balances with better approximation. A distinctive feature of this model is its spatial granularity: the 20 Italian regions are described with their own characteristics and interact by exchanging energy commodities.

Figure 1. Map of Italy with the regions names.

For simplicity, in this thesis the Italian regions are identified by a three-letter code, consistent with the internal labelling of the model, as reported in Table 1.

Table 1. Name and related label for each Italian region.

Region label	Region name
ABR	Abruzzo
BAS	Basilicata
CAL	Calabria
CAM	Campania
EMR	Emilia-Romagna
FVG	Friuli-Venezia Giulia
LAZ	Lazio
LIG	Liguria
LOM	Lombardia
MAR	Marche
MOL	Molise
PIE	Piemonte
PUG	Puglia
SAR	Sardegna
SIC	Sicilia
TOS	Toscana
TAA	Trentino-Alto Adige
UMB	Umbria
VDA	Valle d'Aosta
VEN	Veneto

The model includes two key components: the power sector and the upstream sector which can be divided in a fuel supply Section, and in the hydrogen supply chain. The power sector delivers centralized and distributed electricity, as well as heat. The upstream sector encompasses both the production of energy commodities and foreign trade through import and export activities. All sectors generate emission commodities such as CO_2, CH_4, and N_2O, with CO_2 also serving as a potential input for the production of synthetic fuels .

The technologies in the model are described by the following techno-economical parameters:

a. Input and output commodities.
b. Input and output fuel shares.
c. Efficiency.
d. Existing capacity at the base year.
e. Investment cost.
f. Fixed operation and maintenance (O&M) cost.
g. Variable O&M cost.
h. Capacity factor.
i. Emission activity.
j. Material intensity.

Furtherly, technologies are classified as either existing or new. Existing technologies are those already present in the base year, with an existing capacity assigned in 2022 following energy balances by Terna [38]. Specific constraints are included in the model to prevent new capacity of existing technologies being deployed and to drive the represent their progressive end-of-life and substitution by investment in new technologies. Given that, no investment costs are provided for existing technologies. The techno-economic parameters of new technologies, on the other hand, are specified from the first year of availability on.

2.1.1 Power generation and storage

This Section presents the structure of the power sector in the multi-regional model and describes the techno-economic characterization of both existing and new technologies within this sector. Lastly the electricity demand profile is discussed.

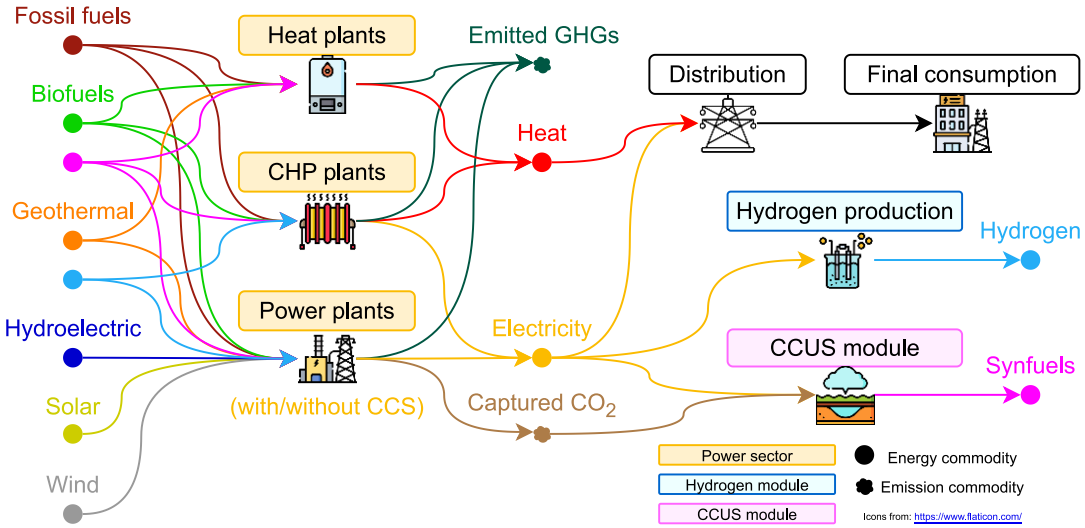

Figure 2. Simplified schema of the power sector structure [40].

Figure 2 illustrates a simplified version of the power sector structure of the model, based on TEMOA-Italy and reproduced in the multi-regional model [28]. There are three types of energy production facilities: power plants producing electricity only, combined heat and power plants (CHP plants) producing both electricity and heat, and heat production plants. Each plant produces one or more energy commodities and may also produce emission commodities.

In addition to meeting final energy service demands, energy commodities are also useful to supply hydrogen production plants and to produce synthetic fuels through carbon capture and storage (CCS) technologies [41]. Although not shown in Figure 2 for clarity, electricity storage plays an essential role in the model's representation of the power sector.

2.1.1.1 Techno-economic characterization and constraints for the power sector

As already mentioned in Section 2.1, the characterization of existing technologies is necessary for model construction. Their description is close to TEMOA-Italy one [42] and it is presented in Table 5. Being 2022 the base year of the multi-regional model, the existing capacity of the technologies for each region is defined from Terna energy balances [38] and it is reported in Table 3. Another useful information is the regional activity of existing technologies in the base year, which is reported in Table 4 [38].

A comprehensive techno-economic description of the new technologies – closely related to the one of TEMOA-Italy model for the power sector – is presented in Table 5. As previously mentioned, energy production technologies are grouped into three main categories: electricity-only generation plants, CHP and micro-CHP facilities (producing both electricity and heat), and heat-only generation units, all of which include a range of technological options. The power sector can utilize various energy inputs, such as fossil fuels (including synthetic fuel blends as discussed in [43], [44]), biofuels, renewable sources, and hydrogen.

The data sources used are listed in Table 5. For CHP, micro-CHP, and heat-only plants, the primary data source is the original version of the TIMES-Italy model [42] except for CHP fuel cells, which follow the JRC-EU-TIMES Model [45].

Table 2. Techno-economic characterization of existing technologies in the model power sector.

Category	Resource	Technology	Efficiency (%)	Variable O&M Cost		Capacity to Activity	Capacity Factor (%)	Capacity Credit (%)	CHPR	Source
Power Plants	Natural Gas	Gas Cycle	42	0.58	M€$_{2022}$/PJ	31.536 PJ/GW	0.02 ÷ 0.8	100		[42] [46]
		Combined Cycle	50	0.47	M€$_{2022}$/PJ		26			
	Coal	Steam Cycle	34	0.38	M€$_{2022}$/PJ		76			
	Oil Products	Steam Cycle	27	0.56	M€$_{2022}$/PJ		24			
	Biofuels	Biodiesel Plant	35	0.42	M€$_{2022}$/PJ		28			
	Hydroelectric	Reservoir		0.09	M€$_{2022}$/PJ	31.536 PJ/GW	≈ 23			[42]
		Run on River			M€$_{2022}$/PJ					
	Geothermal	High Enthalpy Plant	10	4.04	M€$_{2022}$/PJ		81			[42]
	Solar	Photovoltaic		16.11	M€$_{2022}$/PJ	31.536 PJ/GW	≈ 14	20		[42] [46]
	Wind	Onshore					≈ 17	25		
CHP Plants	Natural Gas	Gas Cycle	77	0.58	M€$_{2022}$/PJ	31.536 PJ/GW	39 ÷ 53		≈ 1.3	[42]
		Combined Cycle	71	0.92	M€$_{2022}$/PJ		8.1		≈ 0.6	
		Cycle in Counter Pressure	84	1.61	M€$_{2022}$/PJ		37 ÷ 43		≈ 4.0	
		Cycle with Steam Tapping	80						≈ 2.5	
Micro-CHP Plants	Natural Gas	Internal Combustion Engine (Commercial/ Industry)	55	0.56	M€$_{2022}$/PJ	31.536 PJ/GW	35 ÷ 48	100	≈ 1.1	[42]
Storage	Hydroelectric	Hydro Pumped	80	0.59	M€$_{2009}$/PJ	31.536 PJ/GW				[42]

Table 3. Existing capacity (GW) of existing technologies in 2022 in the different regions.

Category	Resource	Technology	ABR	BAS	CAL	CAM	EMR	FVG	LAZ	LIG	LOM	MAR	MOL	PIE	PUG	SAR	SIC	TAA	TOS	UMB	VDA	VEN
Power Plants	Natural Gas	Gas Cycle	0.02	0.01	0.23	0.00	0.00	0.00	1.05	0.00	0.01	0.00	0.25	0.00	0.11	0.18	0.55	0.00	0.11	0.00	0.00	0.01
		Combined Cycle	0.89	0.00	1.59	2.32	2.35	0.04	1.99	0.78	5.85	0.00	0.78	1.97	1.42	0.04	1.52	0.00	0.44	0.37	0.00	0.00
	Coal	Steam Cycle	0.00	0.00	0.14	0.10	0.08	0.32	1.88	0.00	0.83	0.00	0.03	0.02	1.86	1.11	1.20	0.00	0.03	0.00	0.00	0.75
	Oil Products	Steam Cycle	0.00	0.09	0.00	0.11	0.09	0.04	0.09	0.01	0.22	0.02	0.02	0.11	0.03	0.01	0.17	0.02	0.10	0.01	0.00	0.08
	Biofuels	Biodiesel Plant	0.03	0.08	0.17	0.23	0.60	0.13	0.15	0.02	0.88	0.03	0.04	0.32	0.32	0.10	0.07	0.09	0.15	0.04	0.00	0.31
	Hydroelectric	Reservoir	0.24	0.00	0.28	0.38	0.13	0.16	0.09	0.02	1.84	0.10	0.05	0.61	0.00	0.00	0.12	0.74	0.12	0.37	0.02	0.23
		Run on River	0.56	0.01	0.14	0.44	0.43	0.31	0.31	0.05	2.28	0.11	0.03	1.91	0.00	0.05	0.09	1.75	0.20	0.10	0.76	0.61
	Geothermal	High Enthalpy Plant	0.00	0.00	0.00	0.00	0.00	0.00	0.00	0.00	0.00	0.00	0.00	0.00	0.00	0.00	0.00	0.00	0.77	0.00	0.00	0.00
	Solar	Photovoltaic	0.84	0.41	0.62	1.01	2.51	0.66	1.72	0.15	3.15	1.23	0.19	2.00	3.05	1.14	1.76	0.54	1.02	0.56	0.03	2.49
	Wind	Onshore	0.27	1.46	1.18	1.87	0.04	0.00	0.08	0.12	0.00	0.02	0.40	0.02	2.99	1.09	2.12	0.00	0.14	0.00	0.00	0.01
CHP Plants	Natural Gas	Gas Cycle	0.37	0.03	1.61	0.10	2.66	1.10	0.11	0.00	3.18	0.41	0.00	2.04	2.17	0.59	1.44	0.08	0.72	0.09	0.00	1.67
		Combined Cycle	0.03	0.00	0.00	0.00	0.07	0.00	0.00	0.00	0.17	0.00	0.00	0.03	0.00	0.01	0.13	0.00	0.01	0.00	0.00	0.06
		Cycle in Counter Pressure	0.03	0.00	0.02	0.00	0.31	0.03	0.01	0.00	0.19	0.00	0.00	0.10	0.52	0.22	0.02	0.03	0.07	0.00	0.00	0.07
		Cycle with Steam Tapping	0.00	0.03	0.00	0.02	0.29	0.02	0.07	0.05	0.11	0.00	0.00	0.14	0.02	0.00	0.06	0.03	0.45	0.00	0.00	0.08
Micro-CHP Plants	Natural Gas	Internal Combustion Engine (Commercial/ Industry)	0.12	0.03	0.04	0.12	0.57	0.16	0.24	0.05	1.01	0.06	0.02	0.49	0.07	0.01	0.04	0.13	0.23	0.06	0.01	0.48
Storage	Hydroelectric	Hydro Pumped	0.25	0.12	0.36	0.51	0.09	0.05		0.03	1.99	0.03		1.31		0.41	0.51	0.88	0.05	0.05	0.24	0.33

Table 4. Activity (PJ) of existing technologies in 2022 in the different regions.

Category	Resource	Technology	ABR	BAS	CAL	CAM	EMR	FVG	LAZ	LIG	LOM	MAR	MOL	PIE	PUG	SAR	SIC	TAA	TOS	UMB	VDA	VEN
Power Plants	Natural Gas	Gas Cycle	0.05	0.19	0.06	0.00	0.00	0.00	0.15	0.00	0.17	0.00	0.06	0.00	0.31	0.42	0.70	0.00	0.41	0.00	0.00	0.00
		Combined Cycle	7.30	0.00	11.85	16.45	26.19	1.00	9.75	10.15	63.36	0.00	3.82	21.55	15.58	0.88	6.03	0.00	5.20	2.19	0.00	0.00
	Coal	Steam Cycle	0.00	0.00	4.05	2.39	1.82	2.58	22.54	0.00	4.32	0.00	0.53	0.36	28.16	16.37	16.34	0.00	0.27	0.00	0.00	11.79
	Oil Products	Steam Cycle	0.00	0.65	0.00	2.03	1.20	0.36	0.56	0.05	2.44	0.23	0.26	1.83	0.49	0.24	0.87	0.05	0.56	0.08	0.00	0.94
	Biofuels	Biodiesel Plant	0.26	0.81	4.12	3.51	9.18	2.50	2.05	0.06	13.16	0.46	0.42	5.67	4.37	1.90	0.70	0.88	1.21	0.58	0.00	5.91
	Hydroelectric	Reservoir	0.92	0.00	1.12	0.67	0.37	0.94	0.59	0.07	7.31	0.51	0.38	2.36	0.00	0.00	0.25	4.94	0.42	2.67	0.14	1.72
		Run on River	2.16	0.11	0.57	0.77	1.24	1.90	2.04	0.16	9.04	0.60	0.23	7.42	0.00	0.15	0.18	11.76	0.68	0.70	6.43	4.61
	Geothermal	High Enthalpy Plant	0.00	0.00	0.00	0.00	0.00	0.00	0.00	0.00	0.00	0.00	0.00	0.00	0.00	0.00	0.00	0.00	19.62	0.00	0.00	0.00
	Solar	Photovoltaic	3.49	1.88	2.64	3.86	9.28	2.43	7.34	0.50	10.61	5.08	0.83	7.46	14.79	4.78	7.69	1.90	3.79	2.14	0.11	9.02
	Wind	Onshore	1.57	10.06	7.85	12.13	0.27	0.00	0.50	0.73	0.00	0.12	2.27	0.09	19.09	5.93	11.50	0.00	0.88	0.00	0.00	0.08
CHP Plants	Natural Gas	Gas Cycle	1.13	0.75	25.53	0.12	37.91	20.24	3.30	0.00	63.60	1.18	0.00	51.18	42.84	19.54	40.49	3.43	16.62	0.03	0.00	16.78
		Combined Cycle	0.90	0.00	0.00	0.00	1.03	0.00	0.00	0.00	7.33	0.00	0.00	0.75	0.00	1.42	0.00	0.00	0.09	0.00	0.00	2.68
		Cycle in Counter Pressure	0.41	0.00	0.28	0.00	8.60	1.32	0.52	0.00	7.66	0.00	0.00	4.36	6.76	4.09	0.86	1.22	0.16	0.00	0.00	2.98
		Cycle with Steam Tapping	0.00	0.82	0.00	0.98	11.53	0.87	2.47	1.48	3.58	0.00	0.00	6.95	1.21	0.00	5.62	1.86	16.50	0.00	0.00	3.66
Micro-CHP Plants	Natural Gas	Internal Combustion Engine (Commercial/ Industry)	2.71	0.57	0.67	3.59	17.20	3.84	5.84	1.41	33.79	1.52	0.79	14.20	1.22	0.25	0.65	4.71	5.68	1.77	0.24	15.12
Storage	Hydroelectric	Hydro Pumped	0.96	0.93	1.41	0.89	0.25	0.32		0.09	7.91	0.19		5.09		1.35	1.03	5.89	0.18	0.35	2.04	2.53

Table 5. Techno-economic characterization of new technologies in the model power sector.

Category	Resource	Technology	Efficiency (%)	Lifetime	Investment Cost		Fixed O&M Cost		Variable O&M Cost		Discount Rate (%)	Capacity to Activity	Capacity Factor (%)	Capacity Credit (%)	CHPR	Source
Power Plants	Natural Gas	Gas Cycle	35 ÷ 49	30	703 ÷ 922	M$$_{2020}$$/GW	21	M$$_{2020}$$/GW	1.39	M$$_{2020}$$/PJ	2.7	31.536 PJ/GW	95	100		[42] [46] [47]
		Combined Cycle	54 ÷ 59	30	838 ÷ 1038	M$$_{2020}$$/GW	28	M$$_{2020}$$/GW	0.56	M$$_{2020}$$/PJ			90			
		95% CCS	55	30	1330	M€$$_{2010}$$/GW	38	M€$$_{2010}$$/GW	0.34	M€$$_{2010}$$/PJ			90			
	Coal	Steam Cycle	40 ÷ 44	30	2240 ÷ 3075	M$$_{2020}$$/GW	74	M$$_{2020}$$/GW	2.22	M$$_{2020}$$/PJ	6.2		76			
		79 ÷ 84 % CCS	41 ÷ 48	15 ÷ 30	2757 ÷ 3758	M€$$_{2010}$$/GW	69 ÷ 88	M€$$_{2010}$$/GW	0.64 ÷ 1.62	M€$$_{2010}$$/PJ			90			
	Oil Products	Steam Cycle	40 ÷ 44	30	2240 ÷ 3075	M$$_{2020}$$/GW	74	M$$_{2020}$$/GW	2.22	M$$_{2020}$$/PJ	6.2		85			
		Biodiesel Plant	35 ÷ 39	15	3626 ÷ 4416	M$$_{2020}$$/GW	151	M$$_{2020}$$/GW	1.61	M$$_{2020}$$/PJ	6.7		70			
	Biofuels	Biomass Plant	25 ÷ 28	15	3626 ÷ 4416	M$$_{2020}$$/GW	151	M$$_{2020}$$/GW	1.61	M$$_{2020}$$/PJ			57			
		Agriculture and Farming Biogas Plant	32 ÷ 40	9	2025 ÷ 3500	M€$$_{2009}$$/GW							58 ÷ 65	100		[42]
		Landfill Biogas Plant			900 ÷ 1100	M€$$_{2009}$$/GW	40 ÷ 75	M€$$_{2009}$$/GW	1.61	M€$$_{2009}$$/PJ			49 ÷ 60	100		
	Hydroelectric	Micro-hydroelectric		30	4500	M€$$_{2009}$$/GW	78	M€$$_{2009}$$/GW			5.2		≈ 23	50		[42]
		Mini-hydroelectric			2250	M€$$_{2009}$$/GW	33	M€$$_{2009}$$/GW								
	Geothermal	High Enthalpy Plant	10	15	3200 ÷ 4000	M€$$_{2009}$$/GW	60 ÷ 86	M€$$_{2009}$$/GW			5.2		86	100		[42]
		Low Enthalpy Plant			4480 ÷ 6000	M€$$_{2009}$$/GW							88 ÷ 90	100		
	Solar	Ground Photovoltaic		30	620 ÷ 6000	M$$_{2020}$$/GW	13 ÷ 43	M$$_{2020}$$/GW			5.7		≈ 14	20		[42]
		Rooftop Photovoltaic			751 ÷ 8000	M$$_{2020}$$/GW	10 ÷ 48	M$$_{2020}$$/GW						15		[46] [47]
	Wind	Onshore		20	765 ÷ 2532	M$$_{2020}$$/GW	33 ÷ 49	M$$_{2020}$$/GW			7.6		≈ 17	25		[42]
		Offshore (Fixed)			2343 ÷ 5000	M$$_{2020}$$/GW	70 ÷ 111	M$$_{2020}$$/GW			8.6			30		[46]
		Offshore (Floating)			3467 ÷ 4049	M$$_{2020}$$/GW	57 ÷ 69	M$$_{2020}$$/GW						35		[47]
	Hydrogen	PEM Fuel Cell	45 ÷ 47	15	1000 ÷ 3000	M€$$_{2013}$$/GW	56 ÷ 61	M€$$_{2013}$$/GW	8.33 ÷ 29.17	M€$$_{2013}$$/PJ	8.0		90	100		[45]
	Nuclear	Light Water Reactor		60	5000 ÷ 5600	M$$_{2020}$$/GW	146.96	M$$_{2020}$$/GW	2.92	M$$_{2020}$$/PJ	10.0		94	100		[46]
		Small Modular Reactor		60	5500 ÷ 6200	M$$_{2020}$$/GW	114.00	M$$_{2020}$$/GW	3.13	M$$_{2020}$$/PJ						
CHP Plants	Natural Gas	Gas Cycle	77 ÷ 86	25	960	M€$$_{2009}$$/GW			1.11 ÷ 1.67	M€$$_{2009}$$/PJ	2.7	31.536 PJ/GW	57	70	≈ 1.3	[42]
		Combined Cycle	90	30	720	M€$$_{2009}$$/GW			0.33 ÷ 0.50	M€$$_{2009}$$/PJ			34		≈ 0.6	
		Cycle in Counter Pressure	84	35	702	M€$$_{2009}$$/GW			1.39	M€$$_{2009}$$/PJ			74		≈ 4.0	
		Cycle with Steam Tapping	82	35											≈ 2.5	
	Municipal Waste	Municipal Waste Cycle	38	20	2059 ÷ 4000	M€$$_{2009}$$/GW			9.50 ÷ 12.50	M€$$_{2009}$$/PJ	6.7		70 ÷ 80		≈ 0.5	
Micro-CHP Plants	Natural Gas	Internal Combustion Engine (Commercial)	80 ÷ 88	15	900 ÷ 1100	M€$$_{2009}$$/GW			4.17	M€$$_{2009}$$/PJ	5.0	31.536 PJ/GW	34	20	≈ 1.1	[42]
		Microturbine (Commercial)	80 ÷ 88	12 ÷ 20	1000 ÷ 1500	M€$$_{2009}$$/GW			2.78	M€$$_{2009}$$/PJ			34		≈ 0.4	
		Combined Cycle (Commercial)	80	15 ÷ 20	1300	M€$$_{2009}$$/GW			5.00	M€$$_{2009}$$/PJ			34		≈ 0.4	
		Solid Oxide Fuel Cell (Commercial)	90 ÷ 96	20	2250 ÷ 10000	M€$$_{2020}$$/GW			4.86 ÷ 30.56	M€$$_{2020}$$/PJ			90		≈ 0.4	[45]
	Biofuels	Internal Combustion Engine (Commercial)	80	15	1350 ÷ 1870	M€$$_{2009}$$/GW			4.17	M€$$_{2009}$$/PJ			34		≈ 0.4	[42]
	Hydrogen	PEM Fuel Cell (Commercial)	94 ÷ 96	20	1050 ÷ 1500	M€$$_{2020}$$/GW			6.94 ÷ 13.89	M€$$_{2020}$$/PJ			90		≈ 0.8	[45]
	Natural Gas	Internal Combustion Engine (Residential)	80 ÷ 88	15	900 ÷ 1100	M€$$_{2009}$$/GW			2.78 ÷ 4.17	M€$$_{2009}$$/PJ			34		≈ 1.1	[42]
		Microturbine (Residential)	80 ÷ 92	12 ÷ 20	1000 ÷ 1500	M€$$_{2009}$$/GW			1.67 ÷ 2.78	M€$$_{2009}$$/PJ			34		≈ 1.5	
		Combined Cycle (Residential)	80	15 ÷ 20	1300	M€$$_{2009}$$/GW			0.42 ÷ 0.50	M€$$_{2009}$$/PJ			34		≈ 0.4	
		Stirling Engine (Residential)	80 ÷ 90	15	2100 ÷ 2180	M€$$_{2009}$$/GW			2.78 ÷ 5.00	M€$$_{2009}$$/PJ			34		≈ 0.2	
		Solid Oxide Fuel Cell (Residential)	90	20	3500 ÷ 10000	M€$$_{2020}$$/GW			6.97 ÷ 27.78	M€$$_{2020}$$/PJ			90		≈ 0.5	[45]
	Hydrogen	PEM Fuel Cell (Residential)	92 ÷ 96	20	4000 ÷ 6000	M€$$_{2020}$$/GW			6.94 ÷ 20.89	M€$$_{2020}$$/PJ			90		≈ 0.5	
	Natural Gas	Internal Combustion Engine (Industry)	80 ÷ 91	15	1030 ÷ 1100	M€$$_{2009}$$/GW			2.78 ÷ 4.17	M€$$_{2009}$$/PJ			57	100	≈ 1.1	[42]
		Gas Turbine (Industry)	74 ÷ 80	20 ÷ 25	800	M€$$_{2009}$$/GW			1.39 ÷ 1.67	M€$$_{2009}$$/PJ			74		≈ 1.2	
		Steam Turbine (Industry)	75 ÷ 79	30	1500	M€$$_{2009}$$/GW							63		≈ 0.3	
	Biofuels	Internal Combustion Engine (Industry)	85 ÷ 93	15	1800 ÷ 2100	M€$$_{2009}$$/GW			2.50 ÷ 3.75	M€$$_{2009}$$/PJ			57		≈ 0.2	
Heat Plants	Natural Gas	Natural Gas Plant	80	60	4	M€$$_{2009}$$/PJ	2.4	M€$$_{2009}$$/PJ			5.0	1.00 PJ/PJ	60	100		[42]
	Coal	Coal Plant			6	M€$$_{2009}$$/PJ	2.8	M€$$_{2009}$$/PJ								
	Oil Products	Oil Products Plant			5	M€$$_{2009}$$/PJ	2.5	M€$$_{2009}$$/PJ								
	Biofuels	Biofuels Plant			6	M€$$_{2009}$$/PJ	2.8	M€$$_{2009}$$/PJ								
	Geothermal	High Enthalpy Plant	10		12	M€$$_{2009}$$/PJ	2.5	M€$$_{2009}$$/PJ								
		Low Enthalpy Plant			12	M€$$_{2009}$$/PJ	2.5	M€$$_{2009}$$/PJ								
Storage	Lithium-Ion Batteries	Centralized	85	15	799 ÷ 2170	M$$_{2020}$$/GW	20.2 ÷ 54.6	M$$_{2020}$$/GW			8.0	31.536 PJ/GW		70		
		Distributed			882 ÷ 2525	M$$_{2020}$$/GW	22 ÷ 63.4	M$$_{2020}$$/GW								
	Vanadium-Redox-Flow Batteries	Centralized	65	12	1257 ÷ 1960	M$$_{2020}$$/GW	3.78 ÷ 5.63	M$$_{2020}$$/GW								
		Distributed			1354 ÷ 2093	M$$_{2020}$$/GW	3.96 ÷ 5.98	M$$_{2020}$$/GW								

For power plants, data were gathered from multiple sources, while being discount rates and capacity credits highly context-dependent, values were adopted from the TEMOA-Italy model [42] to better represent Italian characteristics. Table 5 presents the average capacity factors (CFs) for hydro, solar, and wind technologies, but their values vary depending on both intra-annual time slices and regional conditions. Parameters for hydroelectric, geothermal, and biogas plants are drawn from TEMOA-Italy, while information regarding CCS-integrated power plants and hydrogen fuel cells comes from the JRC-EU-TIMES Model [45]. For fossil fuel, solid biomass, solar, and wind plants, data on cost and efficiency are sourced from NREL's 2022 Annual Technology Baseline [46], with plant lifespans based on [47]. Fossil-fuel plant efficiencies are assumed to improve by 10%, from 2025 to 2050, reflecting the trends identified in TEMOA-Italy. Concerning storage systems, the storage duration is assumed of 10 h for hydroelectric pumped storage systems and of 6 h for Lithium Ion batteries and for Vanadium-Redox-Flow Batteries [48].

Potential new investments in electricity import and export capacity are included, with an assumed investment cost of 1000 M€/GW, based on recent projects [49]. By 2050, the capacity is projected to reach approximately 15 GW for imports and around 9 GW for exports, following the historical growth trend outlined in [50].

For capacity factor estimation, historical weather and generation data are needed. In the case of Italy, historical data for solar and wind CFs are taken from the EMHIRES dataset [51], developed by the European Commission's Joint Research Centre (JRC). This dataset provides hourly CF data from January 1st, 1986, to December 31st, 2015, available at various spatial resolution. The data complies with the nomenclature of territorial units for statistics (NUTS) by Eurostat [52]: countries, NUTS1 (macro-regions), and NUTS2 (administrative regions). For this analysis, NUTS2 regional data are used. Hydroelectric CFs are calculated using monthly electricity reports published by TERNA from 2006 to 2022 [53].

In the multi-regional model developed for this thesis, CFs are also used for modeling the regional distribution of renewable resources along Italy. The average annual CF throughout the year for photovoltaic, wind and hydroelectric technologies is consistent with Terna energy balances [38]. Detailed seasonal hourly profiles for wind, solar and hydric resources are obtained combining the information on the average CF for each region from [38] and the seasonal hourly CF profiles from [51] and [53]. These data are displayed in Figure 3 for solar, Figure 4 for wind and Figure 5 for hydroelectric.

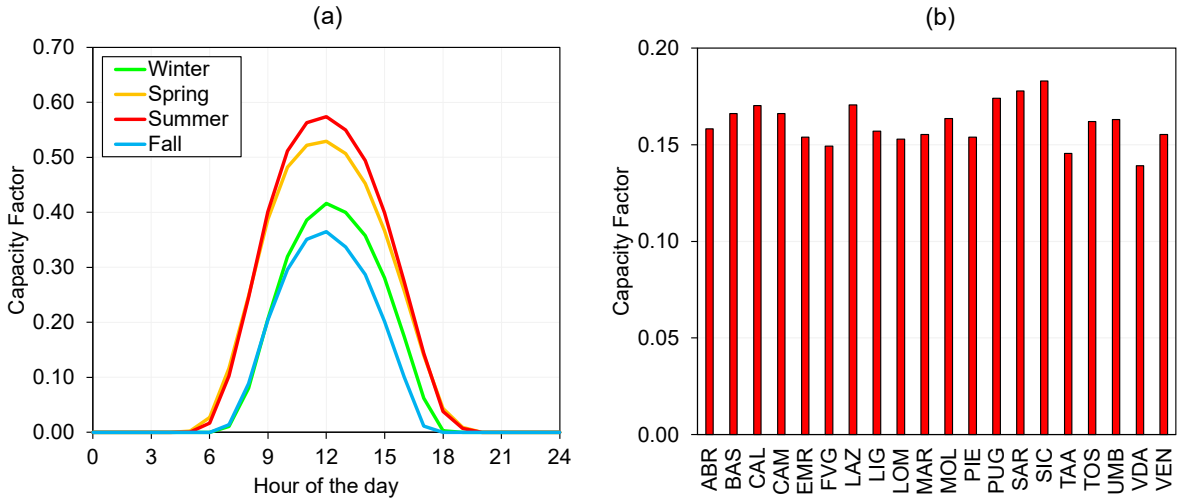

Figure 3. Seasonal daily profiles for Italian CF (a) and average annual CFs for solar resource in the different regions (b).

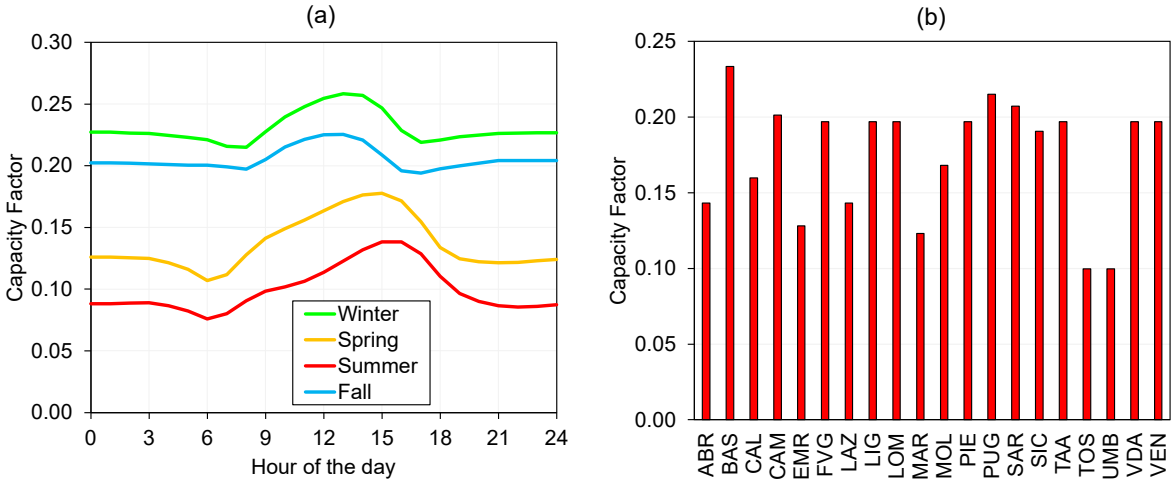

Figure 4. Seasonal daily profiles for Italian CF (a) and average regional CFs for wind resource in the different regions (b).

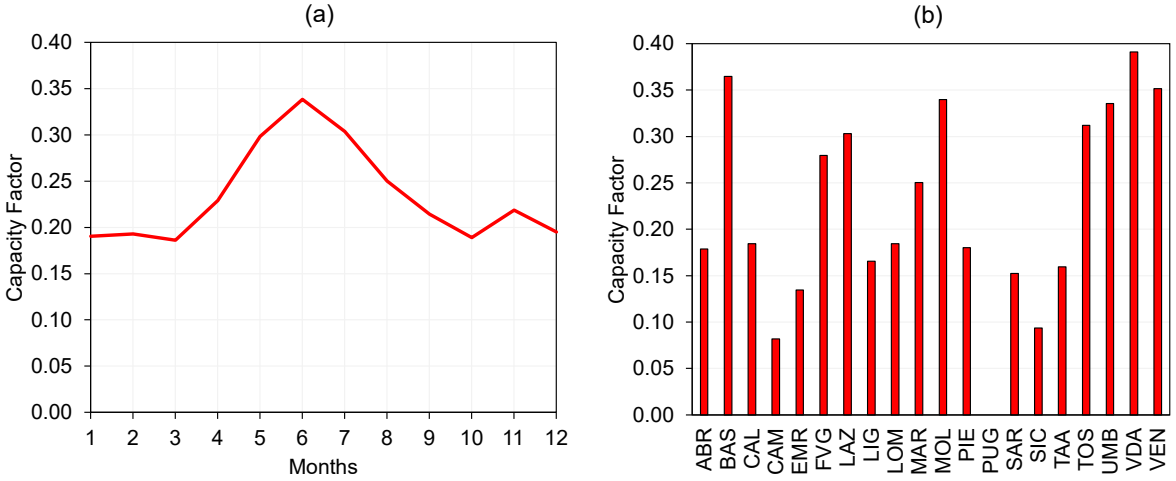

Figure 5. Seasonal daily profiles for Italian CF (a) and average regional CFs for hydroelectric resource in the different regions (b).

On an annual average basis, CFs are approximately 14% for solar and 17% for wind, as also reported in Table 5. For hydroelectric generation, the annual average CF is around 23%, as shown in Table 5. Although the annual hydroelectric CFs from 2006 to 2022 has been showing a slight downward trend, likely due to recent water shortages (especially in 2022 [35]), the model assumes average CF values from 2006–2022 remain constant in the future, anticipating that advances in plant efficiency may offset declining water availability.

Figure 3b, Figure 4b and Figure 5b highlight the differences between resource availability across regions. Solar resource is relatively uniformly distributed throughout the Italian territory, with CF values increasing from north to south. Wind resource exhibit greater spatial variability: central regions are the ones with lowest CFs, while northern and southern ones are more resourceful. The hydric resource presents the highest variability, with zero potential in Puglia and the highest CFs in regions with large basins or rivers, such as Valle d'Aosta, Basilicata and Veneto. The higher the regional variability, the more simplified the resource representation is in a national lumped-parameter model.

At the same time, it is important to account for other regional characteristics that CFs alone cannot capture. For example, although wind resources in the northern regions have higher CFs than

solar, wind still plays a limited role in their current electricity mix. Besides cost-related factors, land availability and social acceptance strongly influence the regional electricity mix [54]. Thus, a complete shift in a region's electricity mix cannot be justified solely by small differences in CFs.

To reflect this, a constraint regarding capacity expansion of renewables is introduced, specifically regarding the share between solar and wind in each region. Data from Terna for solar and wind generation in 2022 is used to calculate the regional energy shares from both sources. A minimum share constraint is then applied across all solar and wind technologies from 2025 to 2050, as reported in Equation 1, where x_r is the share of solar activity in 2022 and $y_r = 1 - x_r$ the share of wind activity in 2022 for each region r.

$$MinShare(x_r) = \begin{cases} 0.75 \cdot x_r, & x_r < 0.9 \\ 0.9, & x_r \geq 0.9 \end{cases}$$

$$MinShare(y_r) = \begin{cases} 0.75 \cdot y_r, & x_r < 0.9 \\ 0, & x_r \geq 0.9 \end{cases} \quad (1)$$

Table 6. Regional minimum shares for solar and wind activity from 2025 to 2050.

Region label	x_r	y_r	$MinShare(x_r)$	$MinShare(y_r)$	Bounded share of solar and wind
ABR	0.69	0.31	0.52	0.23	0.75
BAS	0.16	0.84	0.12	0.63	0.75
CAL	0.25	0.75	0.19	0.56	0.75
CAM	0.24	0.76	0.18	0.57	0.75
EMR	0.97	0.03	0.90	0.00	0.90
FVG	1.00	0.00	0.90	0.00	0.90
LAZ	0.94	0.06	0.90	0.00	0.90
LIG	0.41	0.59	0.31	0.44	0.75
LOM	1.00	0.00	0.90	0.00	0.90
MAR	0.98	0.02	0.90	0.00	0.90
MOL	0.27	0.73	0.20	0.55	0.75
PIE	0.99	0.01	0.90	0.00	0.90
PUG	0.44	0.56	0.33	0.42	0.75
SAR	0.45	0.55	0.33	0.42	0.75
SIC	0.40	0.60	0.30	0.45	0.75
TOS	1.00	0.00	0.90	0.00	0.90
TAA	0.81	0.19	0.61	0.14	0.75
UMB	1.00	0.00	0.90	0.00	0.90
VDA	1.00	0.00	0.90	0.00	0.90
VEN	0.99	0.01	0.90	0.00	0.90

This assumption implies that respectively the 75% or the 90% of the electricity production from solar and wind must respect the minimum shares imposed. As resulting from Table 6, most regions in southern Italy allow a joint deployment of solar and wind, while northern regions primarily depend on solar energy.

Along with technology description, defining a solid set of constraints is essential for model construction. Part of the constraints in TEMOA-Italy and in the multi-regional model are structural constraints. For instance, to define the lifetime of existing technologies, it is introduced a limit on their installed capacity from 2025 on with a decreasing linear trend, making them reach a null generation at

their end of life, with the assumption of constant substitution rate. Moreover, to avoid abrupt changes in the electricity mix from the base year, the activity of each technology in each region in 2025 is bound to be at least 50% of its 2022 level.

INECP [32] is useful to shape policy-based constraints. For example, the capacity of large-scale hydroelectric plants is capped since new installations for these kinds of facilities are not expected [33]. However, the installation of mini and micro hydroelectric plants remains allowed. INECP trajectories [32] along with elaborations from the ENSPRESO database [55] contribute to make estimates concerning the future potential for renewables shaping the constraints on the maximum installable capacity for specific technologies, which is included in Table 7. Significant growth rates are allowed for solar and wind, biomass-fuelled plants and geothermal facilities.

Table 7. Constraints on the maximum installable capacity (GW) of different technologies.

Technology	2025	2030	2040	2050
Biomass Plant	3.32	3.69	4.42	5.15
CHP Municipal waste cycle	0.37	0.46	0.65	0.83
Geothermal high enthalpy	0.25	0.26	0.28	0.30
Geothermal low enthalpy	0.25	0.26	0.28	0.30
Micro-hydroelectric	0.50	0.84	0.82	0.80
Mini-hydroelectric	1.50	2.28	2.32	2.35
Solar photovoltaic ground installation	16.87	33.88	67.90	101.92
Solar photovoltaic rooftop installation	9.15	12.08	17.94	23.80
Wind onshore	14.42	22.67	39.16	55.65
Wind offshore	0.10	2.10	5.25	8.40
Wind deep offshore	0.00	0.00	1.26	6.30

Another policy embedded in the model is the mandated coal phase-out by 2030, as indicated in the Long-Term Strategy (LTS) for greenhouse gas emissions [56], and in the Fit for 55 legislative package [57].

The last set of constraints for power sector is proper of the granularity of the model and regards the regional self-consumption of electricity. The goal is to prevent such an overproduction in resource-rich regions to make others entirely dependent on imports. Therefore, at least 50% of the electricity consumption of each region is bound to be internally produced for each of the milestone years considered. This value is aligned with historical data from Terna regarding electricity generation and consumption by region [38]. Similarly, an upper bound for regional generation from 2025 to 2050 is set. In this case the upper constraint linearly increases from 150% of the 2025 regional electricity consumption in 2030 – aligned with Terna historical data [38] – to 300% of the same value in 2050. This increase in the freedom of the model is consistent with the possibility of expanding the electricity transmission network, as outlined in Section 1.1.

2.1.1.2 Electricity and heat demand distribution

Electricity and heat final demands depend on the considered scenario and include both their final consumption for end-uses (exogenously determined as input data for the model) and possibly additional electricity consumption for hydrogen production (endogenously determined according to the investigated scenario).

The electricity demand profile is characterized by a variable power requested at different times of the day and in different seasons. Since the model temporal resolution compels four typical days, one for each season, the demand curves are obtained averaging yearly data from Terna over the period 2019-2023 about hourly electricity consumption for Italy [58]. In Figure 6 the four hourly demand curves –

one for each season – are represented, normalized to the annual peak load value (occurring at 20:00 of winter). The graph shows a flatter electricity load shape for summer and spring curves, while fall and winter exhibit higher variability between morning, afternoon and evening, with an increase in electricity demand from 17:00 to 20:00. The higher summer electricity demand is mainly due to the use of air conditioning [59].

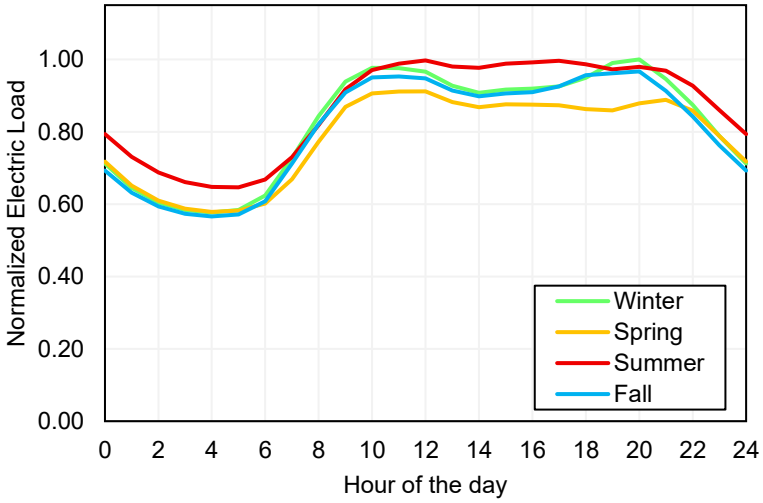

Figure 6. Electricity load profiles in a typical day for each season normalized with respect to the load peak annual value [58].

The load shape for electricity is assumed to be the same across the 20 Italian regions for the four typical days. However, the annual demand level varies by region and its value is obtained from Terna data for 2022 [38]. The regional demand level for both electricity and hydrogen in 2022 is depicted in Figure 7.

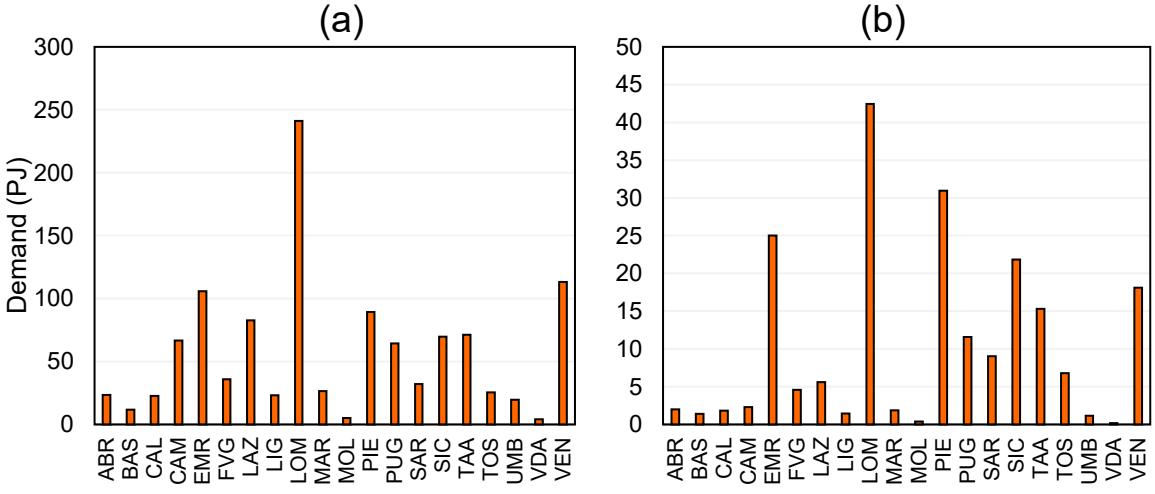

Figure 7. Electricity (a) and heat (b) demand in the Italian regions in 2022 according to Terna [38].

The electricity and heat demand distribution across the 20 regions – which can be observed in Figure 7 – is then used in the scenario definition (Section 2.2) to create shares to project the expected Italian national demand into regional demands. In fact, it is assumed that all Italian regions follow a cohesive trend over the time horizon analysed.

To better frame this assumption, it is useful to compare the data concerning electricity demand shown in Figure 7a to the population density of each region in 2022 [60] and to the regional GDP in the

same year [61]. Specifically, Figure 8 shows the linear correlation of the regional share of electricity demand with both Italian population regional distribution and GDP one.

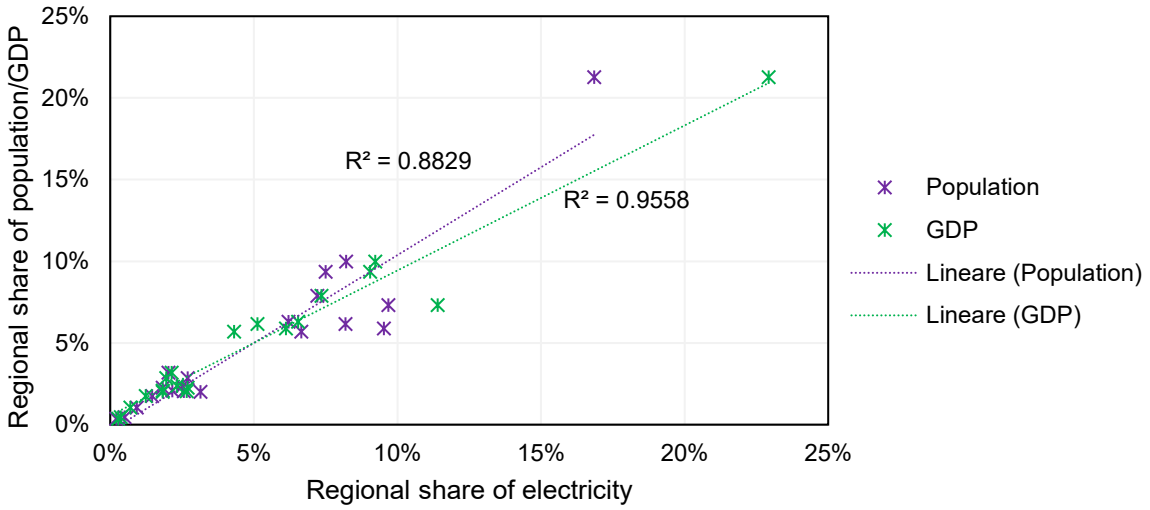

Figure 8. Correlation between electricity demand regional distribution [38] and population [60] and GDP [61] regional distribution in the different regions.

The comparison in Figure 8 highlights the strong linear correlation factor between electricity demand and GDP distribution. At the same time, the correlation between electricity demand and population distribution is still quite high, though a greater number of outliers is visible. Assuming constant regional shares of electricity demand until 2050 implies that the current inequality between northern and southern regions will persist. Bridging this gap will require strong policies and targeted interventions—a topic better addressed through dedicated scenario analyses.

2.1.2 Hydrogen generation and storage

This Section describes the structure of the hydrogen sector in the multi-regional model, classified as a part of the upstream sector and represented in a simplified form in Figure 9. Hydrogen is the commodity produced and used in this sector. Currently, the model considers only hydrogen in gaseous form, since recent scenario analyses performed with TEMOA-Italy (see [62]) do not project a significant liquid hydrogen demand in any sector and because Terna's 2024 SDD mentions liquid hydrogen only as a potential storage solution [33].

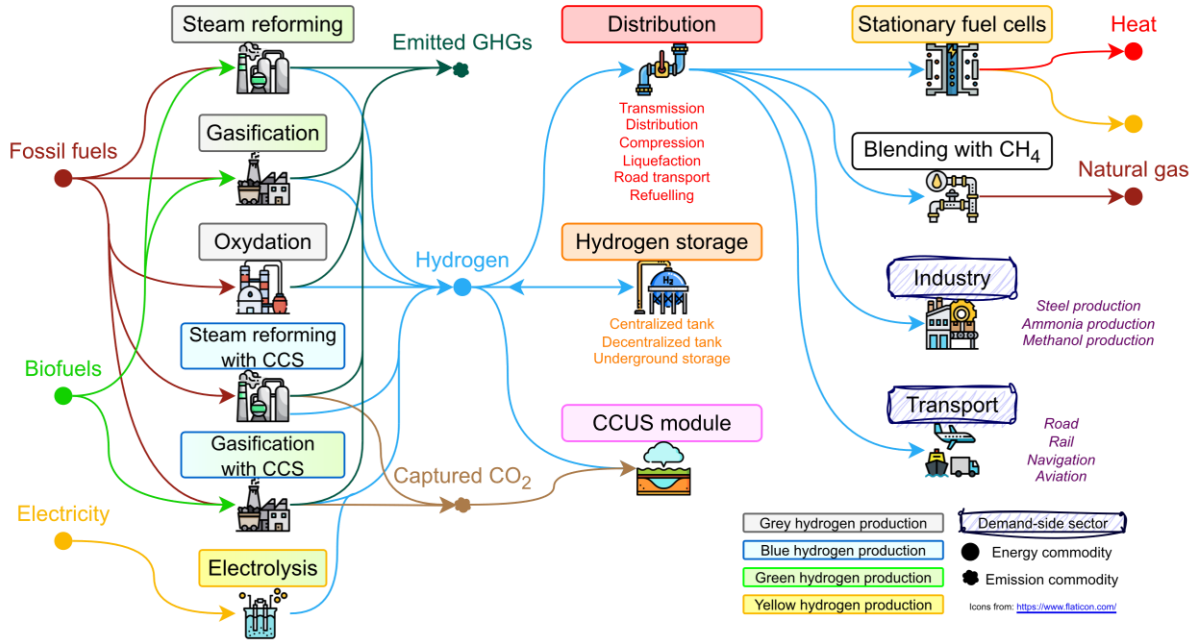

Figure 9. Simplified scheme of hydrogen sector in the model [63].

Figure 9 shows different hydrogen production facilities, classified based on their input sources and on the potential inclusion of carbon capture. The hydrogen colour-based classification is presented in Figure 10, even though it is important to note that each facility does not necessarily belong strictly to only one category.

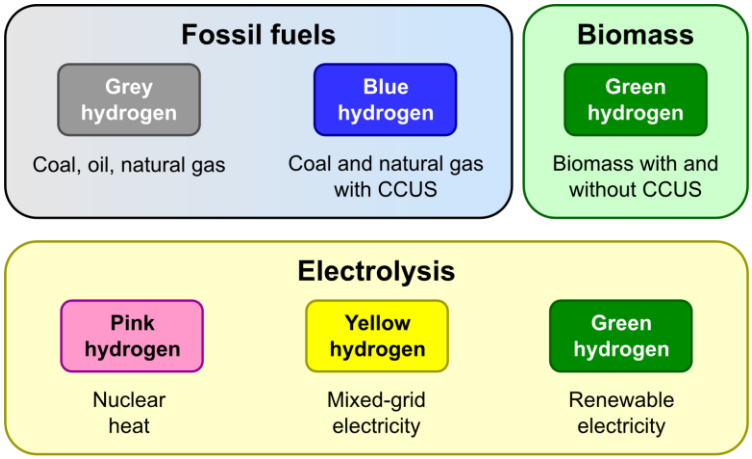

Figure 10. Colour-based classification of the hydrogen production technologies included in TEMOA-Italy. Except for the pink hydrogen, the colours reflect European Union taxonomy [9].

Hydrogen is then distributed and employed in industrial uses, in the transport sector and for electricity production in stationary fuel cells. It can also help decarbonizing natural gas when blended with fossil methane and other compounds directly in pipelines.

2.1.2.1 Techno-economic characterization and constraints for the hydrogen sector

The hydrogen sector is described from the first future year of the model, since there is no significant final consumption of hydrogen before 2025 according to Eurostat Energy Balances [64] and TEMOA-Italy results [41]. Furthermore, a comprehensive mapping of hydrogen consumption patterns and hydrogen production facilities across Italy is currently lacking [65]. For these reasons, existing technologies are not defined in the model, and it is up to the optimization process to select the technological configuration which meets the demand imposed from 2025 onwards. The techno-

economic characterization of hydrogen production options used for the model developed in the context of this thesis is the same as TEMOA-Italy, as available at [66], described in [43] and presented in Table 8. Technologies are grouped by input resource, with key technical and economical parameters specified.

Table 8. Techno-economic characterization of new technologies for hydrogen production.

Resource	Technology	Efficiency (%)	Lifetime	Investment Cost		Fixed O&M Cost		Variable O&M Cost		Capacity Factor (%)	Sources
Natural gas	Steam reforming	61	20	18.4	M€$_{10}$/PJ	0.77 ÷ 0.81	M€$_{10}$/PJ	0.57	M€$_{10}$/PJ	90	[67]
	Steam reforming with CCUS	63		23.5	M€$_{10}$/PJ	1.33	M€$_{10}$/PJ	0.24	M€$_{10}$/PJ		
Oil	Partial oxidation of heavy oils	73	25	15.6	M€$_{10}$/PJ	0.77	M€$_{10}$/PJ	0.16	M€$_{10}$/PJ		
Coal	Gasification	68	20	16.7 ÷ 18.7	M€$_{10}$/PJ	0.66 ÷ 0.69	M€$_{10}$/PJ	0.19 ÷ 1.22	M€$_{10}$/PJ		
	Gasification with CCUS	60		18.5	M€$_{10}$/PJ	0.91	M€$_{10}$/PJ	0.22	M€$_{10}$/PJ		
Biomass	Steam reforming	71	20	18.8	M€$_{10}$/PJ	0.75	M€$_{10}$/PJ	0.20	M€$_{10}$/PJ		
	Gasification	32		79.3	M€$_{10}$/PJ	2.63	M€$_{10}$/PJ	1.30	M€$_{10}$/PJ		
	Gasification with CCUS	51		47.3	M€$_{10}$/PJ	2.36	M€$_{10}$/PJ	0.52	M€$_{10}$/PJ		
Electricity	Proton exchange membrane (PEM) electrolysis	68	7 ÷ 14	23.6 ÷ 37.5	M€$_{20}$/PJ	0.68 ÷ 1.47	M€$_{20}$/PJ				[68]
	Alkaline electrolysis	67	8 ÷ 14	22.5 ÷ 48.9	M€$_{20}$/PJ	0.71 ÷ 1.13	M€$_{20}$/PJ				
	Solid oxide electrolysis (SOEC) cells	94	3 ÷ 10	32.5 ÷ 47.1	M€$_{20}$/PJ	0.98 ÷ 2.07	M€$_{20}$/PJ				
	Anion exchange membrane (AEM) electrolysis	59	10	35.9	M€$_{20}$/PJ	1.08	M€$_{20}$/PJ				[69]

When two values appear in a single cell, a linear cost projection from 2025 to 2050 is applied. The discount rate is set to 8% [41] for all technologies. The main data source for the characterization of hydrogen production technologies by fossil fuels and biomass is the JRC-EU-TIMES Hydrogen Module developed by the Joint Research Centre (JRC) [67]. To describe the specificities of different types of electrolysis facilities, data from IEA [68] and IRENA [69] have been employed.

2.1.2.2 Hydrogen demand distribution

Unlike for electricity demand, hydrogen regional demand distribution is not clearly known for the base year. The distribution of hydrogen demand is hypothesized to be dependent on the GDP regional distribution. According to the literature [70], [71], weighting methods using different indicators are the best solution to estimate hydrogen demand under spatial disaggregation. However, since disaggregate data for many of the indicators considered is unavailable, GDP is chosen as primary weighting indicator, being the one with the highest relevance [70]. The resulting demand distribution is presented in Figure 11, and it is based on the 2022 regional GDP distribution from Istat [61].

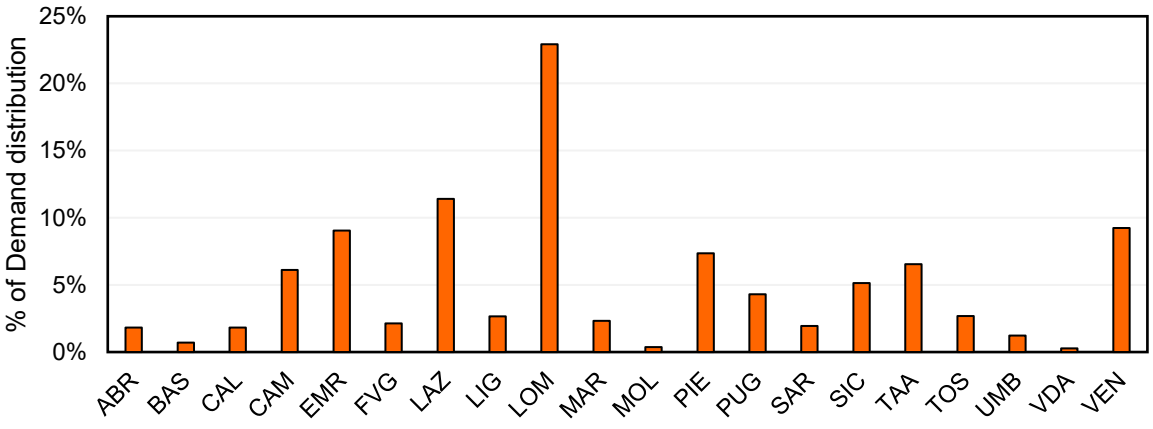

Figure 11. Hydrogen demand distribution for the different Italian regions.

The hydrogen demand distribution is broadly similar to electricity demand: the highest-consuming regions are in the north, with high industrial activity and population density. In this case too, as discussed in Section 2.1.1.2, regional demand distribution is assumed constant over the entire optimization period.

2.1.3 Primary commodities supply and CCUS options

The upstream sector of the model includes both the description of fuel supply and of the CCUS module. The CCUS module – represented in Figure 12 – includes blue hydrogen production technologies, power plants with CCS, and synfuel production options, some of which also exploit hydrogen in the process.

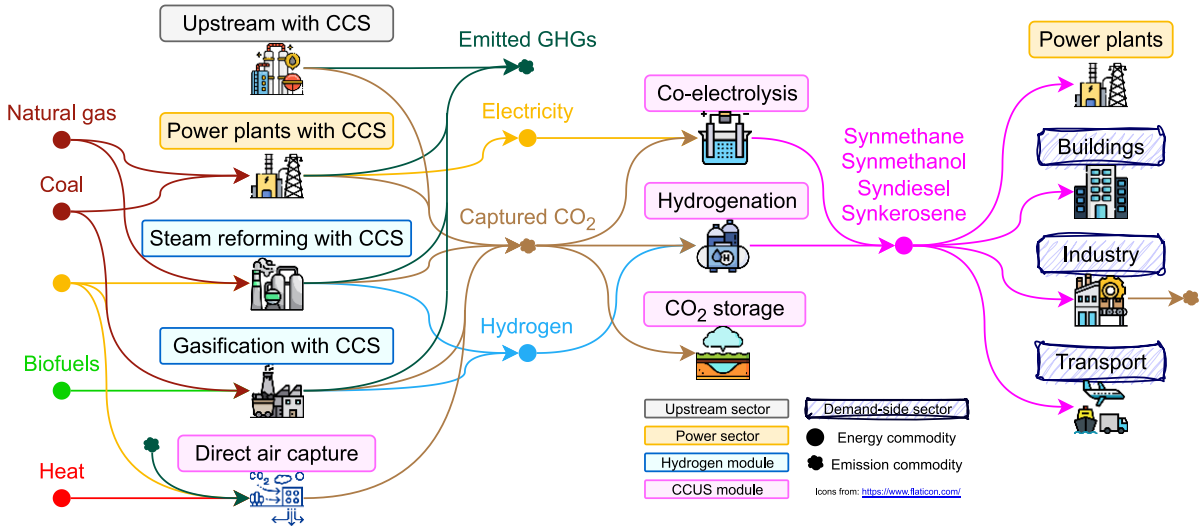

Figure 12. Simplified scheme of CCUS sector in the model [63].

Concerning the part of the model dedicated to fuel supply, a significant part of the upstream sector is dedicated to the biofuels, which includes solid biomass, biodiesel and biomethane [43]. Another important part of the upstream sector consists of the synthetic fuel production.

Part of these fuels are used to decarbonize natural gas: they can be mixed with fossil methane in pipelines respecting the maximum shares shown in Table 9. These constraints are obtained from [72].

Table 9. Fraction of other compounds allowed in natural gas pipelines in the modeled period.

Compound	2025	2030	2040	2050
Synthetic natural gas	0%	5%	53%	100%
Biomethane	1%	5%	53%	100%
Hydrogen for blending	3%	6%	6%	6%

The trade of refined fuels and electricity is modeled through simplified import and export processes characterized by specific trade prices. Import prices for major fossil fuels are shown in Figure 13 and are derived from data reported in [73].

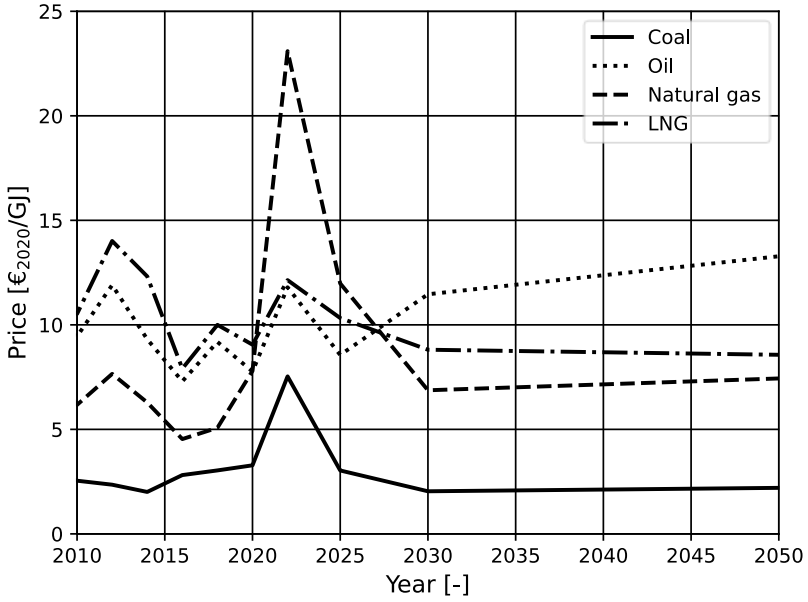

Figure 13. Import prices of coal, oil, natural gas, and LNG modeled in TEMOA-Italy [74].

To each fuel is associated an emission factor, a representative value relating the quantity of a pollutant released to the atmosphere with an activity associated with the release of that pollutant [75]. In this model – as in TEMOA-Italy [28] – the pollutant considered are CO_2, CH_4 and N_2O and the related emission factors are shown in Table 10. Moreover, specific negative emission activities are related to those technology which use implies a direct emission absorption or an indirect emission avoided [72].

Table 10. Emission factors for CO_2, CH_4 and N_2O for the combustion of the fossil fuels considered.

Emission commodity	Coal	Oil	Natural gas
CO_2 (kt/PJ)	101.16	79.55	56.1
CH_4 (kt/PJ)	1.15	0.81	0.13
N_2O (kt/PJ)	1.91	3.18	0.54

The European Emission Trading System (EU ETS) is implemented in the model according to the 2020 European Reference scenario in [76] by applying a carbon tax through an increment of the variable operational cost of fossil fuels import. The carbon tax considered is worth 0.065 M€/t of emitted CO_2 in 2025 and it undergoes a linear growth up to 2050, when it reaches 0.15 M€/t of emitted CO_2 [76]. The emission factor of each fuel is used to convert the carbon tax in a variable operational cost associated to the use of each fuel.

2.1.4 Electricity and hydrogen transport

The modeling of the transmission infrastructure is the key feature of the multi-regional model, as it is essential to characterize the exchange of energy commodities consisting in the way for regions to interact.

2.1.4.1 Transmission distance estimation

The first challenge lies in the definition of the main electricity transmission lines, which is complicated by limited data availability. In fact, Terna provides information only about internal

exchanges between the bidding zones of the electricity market (defined in Table 11), and not about the exchanged power between adjacent regions. The bidding zones are [77]:

a. Northern Italy: Valle D'Aosta, Piemonte, Liguria, Lombardia, Trentino-Alto Adige, Veneto, Friuli-Venezia Giulia, Emilia-Romagna;
b. Central Northern Italy: Toscana e Marche;
c. Central Southern Italy: Lazio, Abruzzo, Umbria e Campania;
d. Southern Italy: Molise, Puglia e Basilicata;
e. Calabria;
f. Sicilia;
g. Sardegna.

Table 11. Transmission capacity (GW) between bidding zones in 2022 from Terna [78].

Interconnected regions		**Transmission capacity**
Northern Italy	Central Northern Italy	3.70
Central Northern Italy	Central Southern Italy	2.85
Central Southern Italy	Southern Italy	3.70
Southern Italy	Calabria	1.73
Calabria	Sicilia	1.40
Central Northern Italy	Sardegna	1.17

Knowing the characteristics of the Italian territory, it would be unrealistic to assume a direct transmission line between each pair of adjacent regions. Natural barriers sometimes prevent or discourage the installation of significant inter-regional lines (e.g. between Marche and Umbria). For this reason, the transmission lines assumed in the model are the ones highlighted in Figure 14.

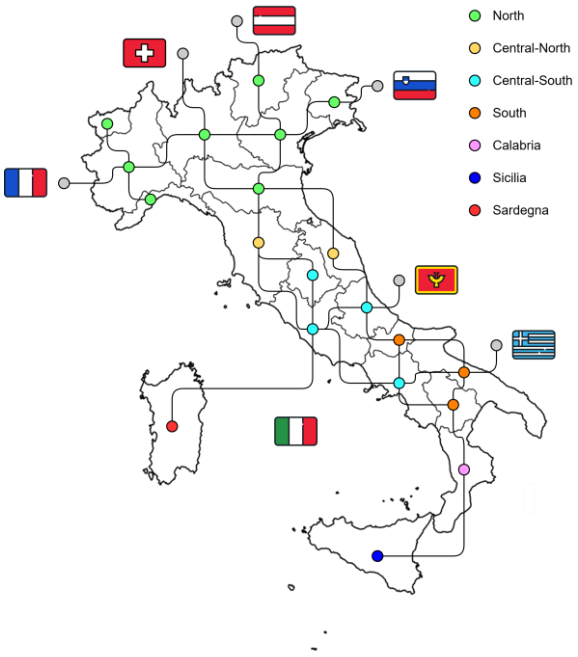

Figure 14. Main electricity transmission lines between adjacent regions.

Next, representative distances for electricity transmission lines between regions are estimated. For each couple of interconnected region, the distance between the centres of the two regions is roughly estimated and associated with three different distance levels, namely 100 km, 150 km and 200 km (selected as proper qualitative representation of the average distance ranges between Italian regions).

As shown in Figure 14, twenty-five transmission lines are identified. Most of them are overhead lines, except for those connecting Lazio to Sardegna and Calabria to Sicily, which are submarine. These line types and distances are used for the techno-economic characterization of both electricity and hydrogen transmission technologies. In fact, most of the parameters of these technologies are distance-dependent and therefore scaled according to the assumed distances.

Although this modeling choice certainly introduces approximations in the estimation of the investment costs for deploying new transmission lines, it should be noticed that this assumption is kept consistent for all the technology options competing for the same transmission lines. Thus, it is expected to not significantly affect the technology competition. Moreover, modeling the electrical connections between adjacent regions with a single line is by itself a simplification of reality induced by the model structure. For these reasons, methodologies to identify more precise expected lengths of transmission lines are out of the scope of this thesis and were not adopted.

2.1.4.2 Electricity transmission characterization

Both existing and new technologies are modeled for electricity transmission. The first represents the current grid configuration: an existing capacity for each transmission line is assumed in the base year, based on regional energy import data [78] and consistent with Terna values in Table 11. The proposed disaggregation of existing capacities between macro-regions into existing capacities between single regions is made based on the historical electricity import/export value of each region and is reported in Table 12. As for the distances between different regions, such existing capacities are characterized by large uncertainties as well, but they are also expected to minorly affect the model results especially in future years far from the beginning of the time horizon, being existing capacity constraints to be disposed of within the technology lifetime span.

Table 12. Assumed existing capacity (GW) for the existing electricity transmission between couples of interconnected regions in 2022.

Interconnected regions		Existing Capacity
ABR	LAZ	1.27
ABR	MAR	0.78
ABR	MOL	0.31
BAS	CAL	1.10
BAS	CAM	0.94
BAS	PUG	1.92
CAL	SIC	1.11
CAM	LAZ	1.90
CAM	MOL	0.94
CAM	PUG	2.64
EMR	LOM	0.59
EMR	MAR	1.08
EMR	TOS	1.02
EMR	VEN	2.31
FVG	VEN	2.43
LAZ	SAR	1.42
LAZ	TOS	1.59
LAZ	UMB	1.39
LIG	PIE	1.69
LOM	PIE	1.63
LOM	VEN	1.91
MOL	PUG	1.92
PIE	VDA	1.70
TAA	VEN	1.93
TOS	UMB	0.85

The new technology still describes the traditional electricity transmission infrastructure but it is available for capacity additions according to the specific future scenario. Existing capacity is progressively phased out, starting with a cap at 80% of the 2022 capacity in 2025 and reaching 0 by 2050. The new technology progressively substitutes the existing one, allowing the model to develop a more flexible system, free from the hypotheses made on the existing capacity of 2022.

The technical parameters of existing and new electricity transmission technologies are identical, while investment costs are defined only for new technologies. The efficiency for each line is calculated by considering power losses of 7%/1000 km as in [79]. In accordance with [80], the investment cost for each overhead line is set at 400 €/km/MW [81] and at 970 €/km/MW [82] for each submarine line (between Sardegna and Lazio and between Sicily and Calabria). For both the line types, the fixed operational and maintenance cost is set to 2% of the specific investment cost and a discount rate of as 5% is applied. The Capacity to Activity ratio – representing a conversion factor from capacity to activity unit of measurement – is of 31.536 PJ/GW.

2.1.4.3 Hydrogen transport characterization

Hydrogen transport is still an innovative technology, hence, its techno-economic characterization carries significant uncertainty. According to the literature [83], [84], gaseous hydrogen transport in pipelines is considered the most cost-effective solution for hydrogen mass flowrates exceeding 150 t/day. Thus, pipelines are the only hydrogen transport technology described in the model.

Alternative transport means consist of hydrogen land transport via trucks or rail, both in compressed gaseous and in liquefied form [83]. The transport of liquid hydrogen is competitive by truck for very low hydrogen mass flowrates, and by rail for long distances and low hydrogen mass flowrates, while gaseous hydrogen one road transport is never competitive [83], [84]. Given the transmission distances and hydrogen demand (as detailed in Section 2.3), pipelines are the most appropriate choice for hydrogen transport in this model.

Hydrogen transport is introduced in the model as a new technology, starting from 2023 like all other hydrogen-related ones. The technology selected for hydrogen transport is a single line 70 bar pipeline, with nominal power in the range 250-500 MW (consistent with both SCEP capacity and the modeled hydrogen demand as in Section 2.3). The information describing this technology is included in a dataset for transmission technologies from the Danish Energy Agency (DEA) [85] for 2020, 2030 and 2050. Values for 2025 are obtained by interpolating the data of 2020 and 2030. The techno-economic characterization of the hydrogen transport pipeline as it is included in the model is reported in Table 13.

Table 13. Techno-economic characterization of hydrogen transport pipeline from [85].

Parameters	2025	2030	2050	Units
Electricity demand for compression	0.89	0.84	0.75	%
Pressure losses	6.1	5.8	5.2	%/1000 km
Investment costs	1.063	1.063	1.063	€/kW/km
Fixed O&M costs	0.404	0.266	0.199	€/km/MW/y

The electricity needs to compress hydrogen are embedded in the technology description and consider a fixed electricity demand for hydrogen compression and a variable electricity demand to cover pressure losses depending on the length of the pipeline. For offshore pipelines, the investment cost values in Table 13 are increased by 40% as resulting from [86].

2.1.4.4 SCEP characterization

The Superconducting Energy Pipeline (SCEP) is modeled as a dual-purpose infrastructure capable of simultaneously transmitting electricity and hydrogen [17]. SCEP is included in the model as a new technology and it is implemented starting from 2025.

The first step consists in determining the electricity and hydrogen shares within the technology. As from [21], the nominal electric power of SCEP is set at 300 MW. The hydrogen mass flowrate, on the other hand, depends on the operating conditions of the pipeline – especially temperature and pressure – as highlighted in Figure 15.

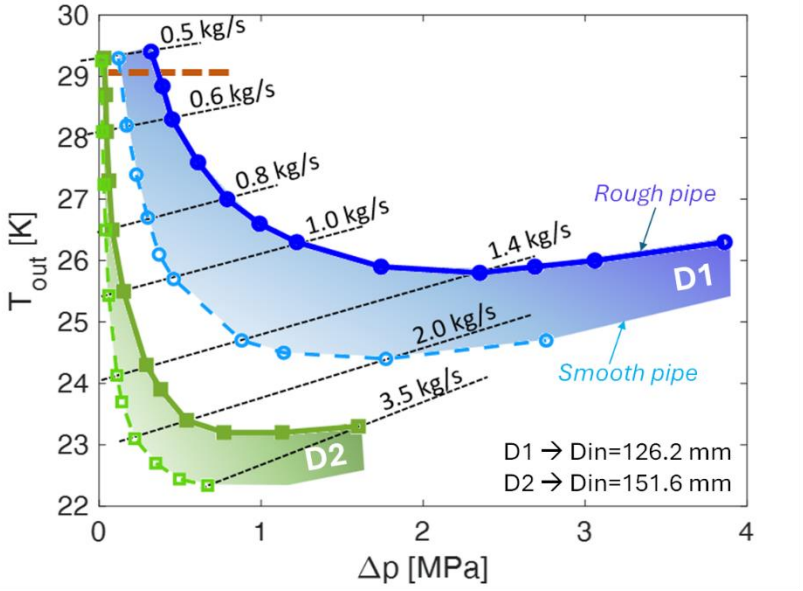

Figure 15. Operation range for the LH_2 pipeline in terms of outlet temperature and pressure drop along the duct. D2 is the corrugated pipe with D_{in} = 126.2 mm, D1 the one with D_{in} = 151.6 mm [21].

As from Figure 15, the hydrogen mass flowrate can vary between 0.6 kg/s and 3.5 kg/s with the respective operating conditions: T_{out}, Δp_{out} of 29 K and 0.8 MPa and T_{out}, Δp_{out} of 23 K and 1.6 MPa. From these mass flowrate values, an equivalent power for hydrogen transport P_{H_2} is determined as reported in Equation 2, where LHV_{H_2} is the lower heating value of hydrogen and $\dot{m}$ is the hydrogen mass flowrate in the pipeline. Then, the power ratio between electricity and hydrogen transport is obtained, which data is included in Table 14.

$$P_{H_2} = LHV_{H_2} * \dot{m} \qquad 2$$

Table 14. Electricity to hydrogen power ratios in SCEP operating range.

Parameters	**T_{out} = 29 K Δp_{out} = 0.8 MPa**	**T_{out} = 23 K Δp_{out} = 1.6 MPa**	**Units**
Electric power	300	300	MW
LHV of H_2	120	120	MJ/kg
H2 mass flowrate	0.6	3.5	kg/s
Equivalent H_2 power	72	420	MW
Electricity to Hydrogen power ratio	4.17	0.71	-

The condition selected to test the cost-competitiveness of SCEP in the Italian power sector is far from the thermodynamic limits. It consists of a mass flowrate of 2 kg/s with a T_{out} between 24 and 25 K and a Δp_{out} of around 1.8 MPa [21]. In this case, an electric power of 300 MW corresponds to an hydrogen equivalent power of 240 MW. The nominal electricity to hydrogen power ratio is 1.25.

SCEP requires the presence of liquid hydrogen for its operation. Since hydrogen liquefaction is an energy-intensive process, it is necessary to consider the electricity input to this process. From literature, current hydrogen liquefaction processes present a specific electricity consumption between 11.9 and 15 kWh/kgLH_2 [87]. Averaging these values and applying the proper conversions, the electricity requirement for the liquefaction process is of 0.404 kWh/kWhLH_2.

The liquefaction process is included in the model as part of SCEP technology, as shown in Figure 16. This liquefaction needs are considered embedded in each segment of the pipeline, considering

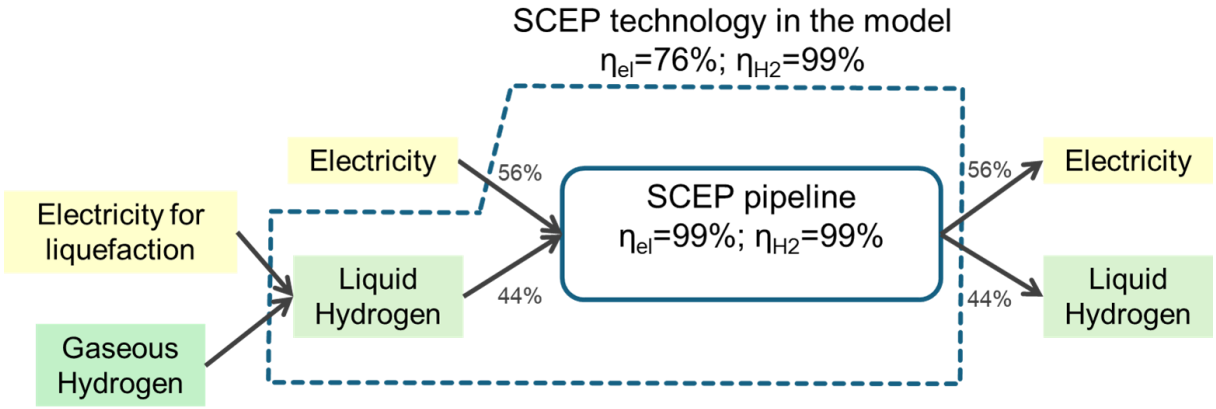

Figure 16. Conceptual structure for modeling SCEP technology with a transmitted hydrogen mass flowrate of 2 kg/s.

From the model perspective – illustrated in Figure 16 – SCEP technology receives electricity and gaseous hydrogen as inputs. The electricity input is divided in two parts: the electricity to be transmitted and the electricity required for hydrogen liquefaction. The electricity used for hydrogen liquefaction is considered as an internal electricity loss in SCEP, and represents the 24% of SCEP electricity input. Being SCEP a closed system, the efficiency of hydrogen transport is assumed to be 99%.

Regarding SCEP cost estimate, an investment cost of 1.1 M€/km is assumed. The cost is scaled on the nominal power of the system – calculated as the sum of the transmitted electric power and of the equivalent hydrogen power – to be correctly included in the model. Consequently, the specific investment costs for traditional electricity transmission [81], [82] and hydrogen transport via pipelines [85], [86], and SCEP one can be compared.

$$CI_{eq} = CI_e * \frac{P_{e_{SCEP}}}{P_{n_{SCEP}}} + CI_{H_2} * \frac{P_{H_{2_{SCEP}}}}{P_{n_{SCEP}}} \qquad 3$$

The comparison is based on the equivalent cost of technologies, calculated using Equation 3 for both the onshore and offshore line configurations, where $CI_{eq;e;H_2}$ are, respectively, the cost investments for the equivalent conventional transmission configuration, traditional electricity transmission and hydrogen transport. $P_{e_{SCEP}}$ and $P_{H_{2_{SCEP}}}$ are the nominal electric and hydrogen equivalent power for SCEP and $P_{n_{SCEP}} = P_{e_{SCEP}} + P_{H_{2_{SCEP}}}$ is the nominal total power of the technology. The outcomes of the cost investment comparison are presented in Figure 17.

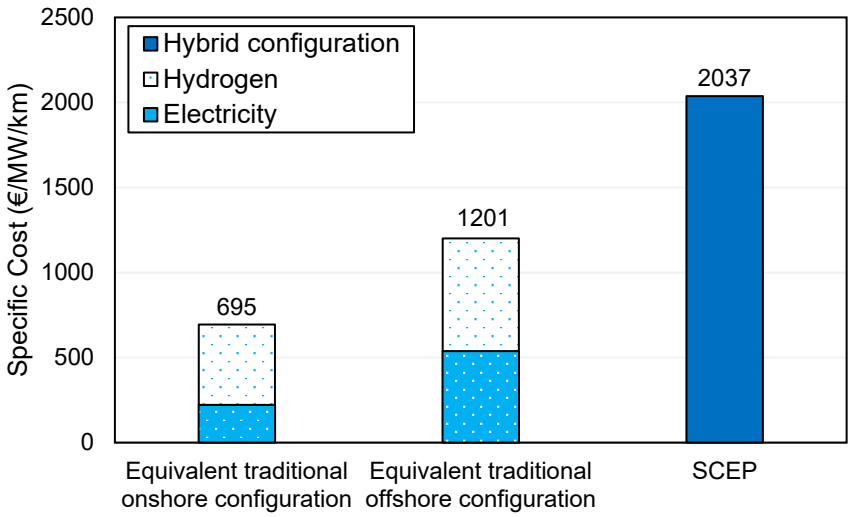

Figure 17. Comparison of specific transmission cost for conventional electricity and hydrogen transmission and SCEP considering a 56% share of electricity and a 44% of hydrogen.

Figure 17 shows the difference between the equivalent specific costs in the different configurations. The offshore configuration costs 1.7 times more than the onshore one. SCEP costs 2.9 times the traditional onshore configuration, and 1.7 times the traditional offshore configuration.

2.2 The investigated scenarios

In this Section are explained the main assumptions used to build the scenario set necessary to test SCEP cost competitiveness. The scenario tree represented in Figure 18 highlights the main variables changing from one scenario to the other.

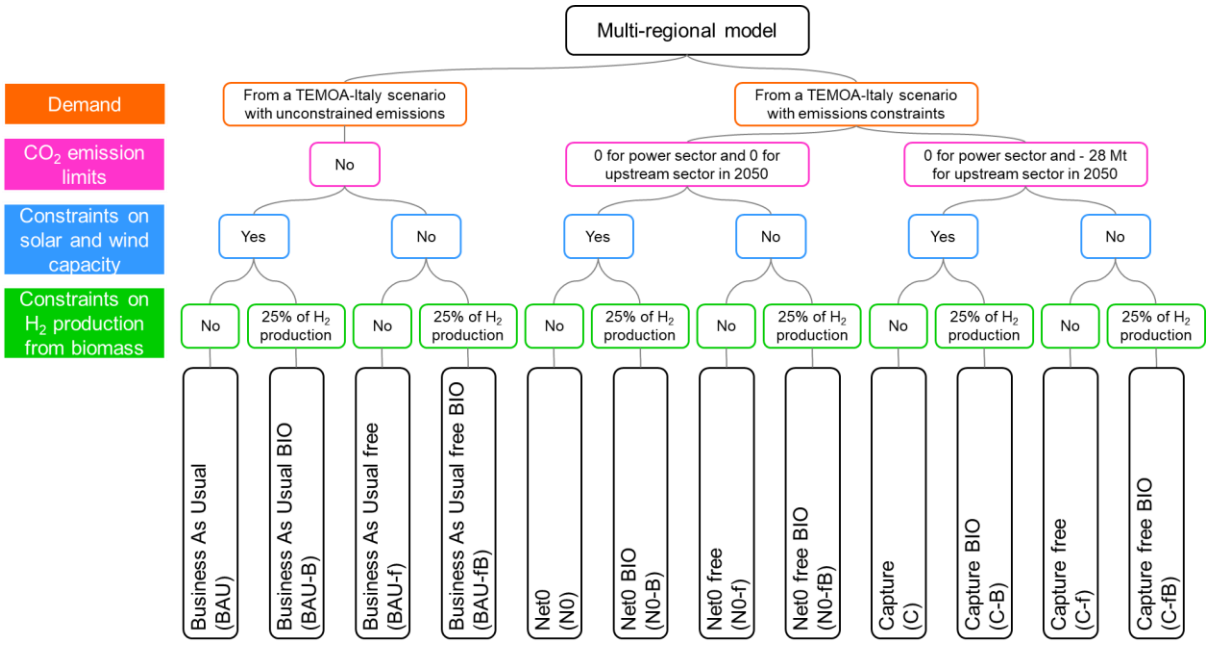

Figure 18. Scenario tree for the multi-regional model to test SCEP cost-effectiveness in the Italian power sector.

As from Figure 18, four levels of assumptions end up creating twelve scenarios for the Italian power and hydrogen sector. According to the results of the optimization, one scenario will be selected to evaluate the cost reduction necessary to have SCEP in the technology mix.

The first set of constraints regards the electricity and hydrogen demand used as an input for the model. The two resulting scenarios groups refer to two different TEMOA-Italy scenarios: the first is a cost-optimal scenario without constraints on emissions, while on the second one is imposed a linearly decreasing CO_2 emission limit from 194 Mt in 2030 to 29 Mt in 2050. Specifically, the trajectory for the latter scenario is obtained from a combination of the Fitfor55 package of the European Green Deal [88] regarding the 2030 constraint and from the Italian Long-Term Strategy for the Reduction of Greenhouse Gases Emissions for 2050 [89].

The demand levels for BAU and N0 and C scenarios are extracted from the results of these two TEMOA-Italy scenarios – respectively the free one and the constrained one concerning emission limits – and are represented in Figure 19.

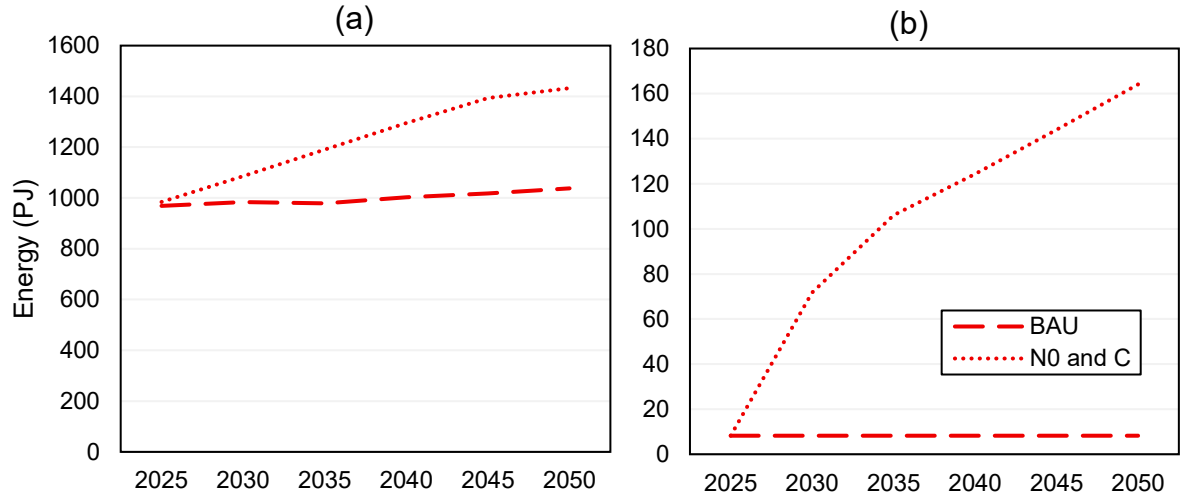

Figure 19. Electricity (a) and hydrogen (b) demand levels for Italy in BAU and in N0 and C scenarios.

The electricity demand in BAU scenario is not varying significantly from 2025 to 2050. Regarding hydrogen, its demand for the BAU scenario is imposed constant and equal to the 2025 hydrogen demand resulting from the TEMOA-Italy scenario with constrained emissions. Concerning N0 and C scenarios, the demand level of electricity steadily grows from 984 PJ in 2025 to 1432 PJ in 2050. Concurrently, the hydrogen demand grows more than 10 times in the interval between 2025 and 2050 since hydrogen is a cost-effective solution for the decarbonization of hard-to abate sectors like transport and industry [41].

To better contextualize and verify the assumptions made in Section 2.1.4.3, the hydrogen mass flowrates corresponding to the total hydrogen demand in the two scenario groups are obtained. The daily hydrogen mass flowrate needed for the BAU group of scenarios is of 188 t/day from 2025 to 2050, while for N0 and C scenarios is between 188 t/day in 2025 and 3747 t/day in 2050.

The demand of each scenario is closely linked to the second constraints group regarding CO_2 emissions. From these two set of constraints, three scenario branches are identified and are presented in Table 15.

Table 15. CO_2 emission limits (Mt) across the scenarios for power and upstream sectors of the multi-regional model.

Scenario	Power sector				Upstream sector			
	2035	2040	2045	2050	2035	2040	2045	2050
Business As Usual (BAU)								
Net 0 (N0)	22.5	12.1	9.7	0	5.8	1.6	0	0
Capture (C)	22.5	12.1	9.7	0	5.8	1.6	-11	-28.1

The emission trajectory for scenarios N0 and C is obtained from the previously cited scenario of TEMOA-Italy. For the power sector, from the emissions resulting from TEMOA-Italy power sector is shaped a constraint applied on the CO_2 emissions of the multi-regional model power sector in both N0 and C scenarios. Concerning the upstream sector, the emission trajectory from TEMOA-Italy is applied to C scenarios, while N0 scenarios do not consider the possibility of having a negative cap for emissions: the minimum emission limit is set at zero.

The third set of constraints consists of imposing a limit in the maximum power of certain categories of technologies that the model can install. In this case the two possible constraints imposed divide scenarios between "constrained" scenarios, and "free" ones. "Constrained" scenarios include the constraints reported in Table 7 for the maximum installable power for solar and wind sources, while for "free" scenarios the constraints of Table 7 are doubled from 2030 on.

The fourth set of constraints impacts on the hydrogen sector since considers a limit in the maximum share of hydrogen that can be produced by biomass. This constraint allow to distinguish "non-BIO" scenarios from "BIO" scenarios. In fact, being biomass both the cheapest fuel for hydrogen producing processes and a low CO_2 emitting one, other production processes hardly enter the technology mix. Consequently, in "BIO" scenarios the hydrogen produced from biomass is bound to be maximum the 25% of the total hydrogen produced.

2.3 Evaluation of SCEP cost-efficiency

To evaluate SCEP cost-efficiency, a scenario is chosen. A sensitivity analysis is performed to determine the minimum cost at which SCEP enters the technology mix. Two parameters are considered:

a. SCEP investment and fixed costs;
b. investment and fixed costs for conventional electricity transmission.

The choice of the first parameter is useful to directly investigate possible effects of the cost reduction of SCEP technology. Investment costs – and consequently fixed costs – vary from the total cost of SCEP to being the 10% of it. This cost decrease is made in ten steps, each representing a 10% of cost reduction with respect to the starting cost estimated.

The second parameter is used to highlight the possible effects of an external factor onto the possibility of installing SCEP. An increase in the cost of metallic materials – mainly aluminium and copper – consequent to an increase in their demand for clean energy technologies [90] causes an increase in the cost of traditional electricity transmission. Specifically, a cost variation of 0%, an increase of 50% and an increase of 100% are considered for traditional electricity transmission.

Table 16 collects the names for the sensitivity scenarios as well as and the ratio between SCEP cost and the traditional equivalent alternative, for both onshore and offshore lines. This ratio is calculated as follows:

$$\frac{SCEP}{TR_{eq}} = \frac{CI_{SCEP} * \Delta CI_{SCEP}}{CI_e * \Delta CI_e * \frac{P_{e\,SCEP}}{P_{n_{SCEP}}} + CI_{H_2} * \frac{P_{H_2\,SCEP}}{P_{n_{SCEP}}}} \qquad 4$$

where $CI_{eq;e;H_2}$ are respectively the cost investments for the equivalent conventional transmission configuration, the cost investment of traditional electricity transmission and the one for hydrogen transport. $\Delta CI_{SCEP;e}$ are respectively the cost decrease in SCEP as in Table 16 and the cost decrease for traditional electricity transmission. $P_{e\,SCEP}$ and $P_{H_2\,SCEP}$ are the nominal electric and hydrogen equivalent power for SCEP and $P_{n_{SCEP}} = P_{e_{SCEP}} + P_{H_2\,SCEP}$ is the nominal total power of the technology.

Table 16. Names for the sensitivity scenarios for different cost levels of SCEP and of traditional electricity transmission.

		Investment cost of Traditional Electricity Transmission		
		100%	**150%**	**200%**
Investment cost of SCEP	**100%**	SCEP100_TR100	SCEP100_TR150	SCEP100_TR200
	90%	SCEP90_TR100	SCEP90_TR150	SCEP90_TR200
	80%	SCEP80_TR100	SCEP80_TR150	SCEP80_TR200
	70%	SCEP70_TR100	SCEP70_TR150	SCEP70_TR200
	60%	SCEP60_TR100	SCEP60_TR150	SCEP60_TR200
	50%	SCEP50_TR100	SCEP50_TR150	SCEP50_TR200
	40%	SCEP40_TR100	SCEP40_TR150	SCEP40_TR200
	30%	SCEP30_TR100	SCEP30_TR150	SCEP30_TR200
	20%	SCEP20_TR100	SCEP20_TR150	SCEP20_TR200
	10%	SCEP10_TR100	SCEP10_TR150	SCEP10_TR200

Chapter 3

Results

3.1 Electricity generation, storage and transmission

This Section presents the results of the scenarios of the model introduced in Section 2.2. The first outcome of the model concerns the electricity generation mix in each scenario. The most relevant results on this aspect are presented in Figure 20 and Figure 21 for 2025, 2030, 2040 and 2050.

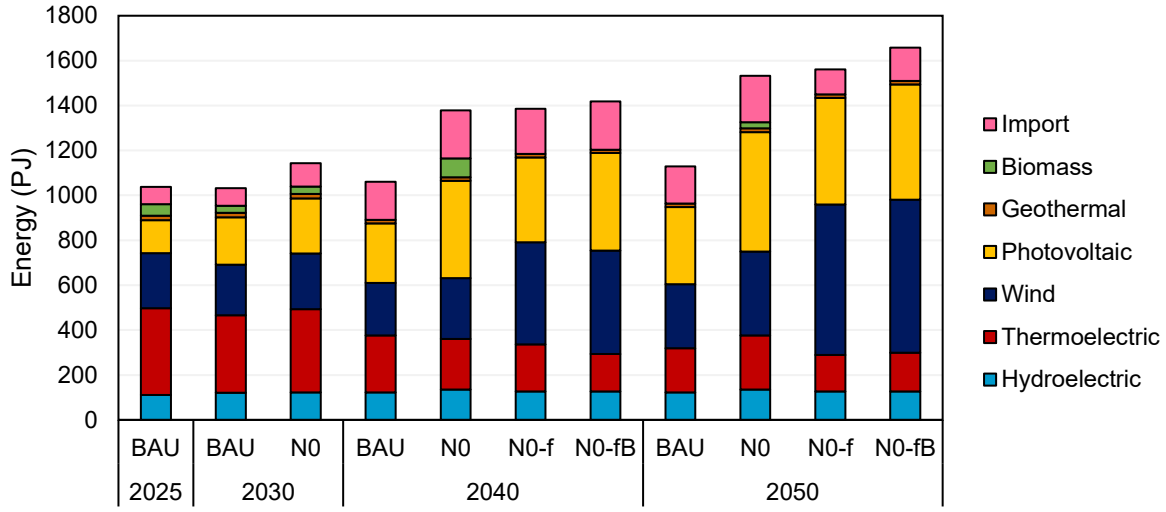

Figure 20. Activity of the electricity mix in some significant scenarios.

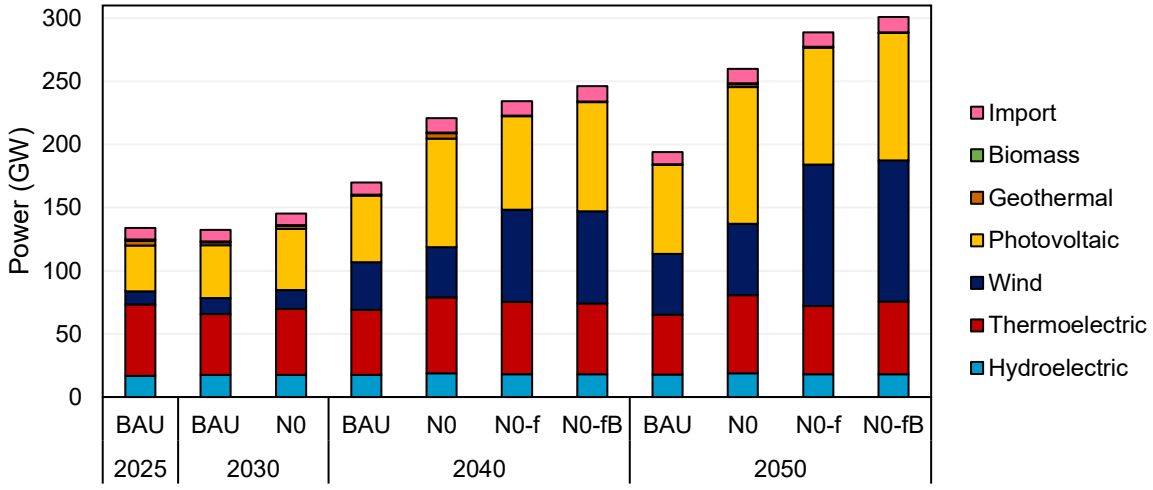

Figure 21. Capacity of the electricity mix in some significant scenarios.

In the BAU scenario, a change in the electricity mix from 2025 to 2050 is reported, driven both by the increase in the efficiency and the decrease in the investment costs of renewable technologies (as in Table 5), and by the increase in the carbon pricing due to the ETS for fossil fuels (as in Section 2.1.3). Specifically, 66% of the electricity in 2050 is expected to be produced from renewable sources, compared to the 24 % in 2022 (from Terna's data [38]). The BAU-B scenario results are not shown since the differences concerning the power sector with respect to those for BAU are negligible, while the main differences lie on hydrogen. The results of BAU-f and BAU-fB scenarios are not commented since they obtain the same results respectively as BAU and BAU-B ones. In fact, in scenarios BAU and

BAU-B the constraints on maximum capacity of solar and wind are not reached, so the model configuration does not benefit from having these constraints loosened.

In the N0 scenario, the capacities of solar, wind and thermoelectric increase with respect to the BAU ones, to sustain the increased electricity demand. From 2030 to 2040, the electricity produced from thermoelectric source decreases to comply with the emission constraints. However, the thermoelectric capacity remains constant to ensure an adequate reserve margin capacity for renewables.

Compared to N0 scenario, both the electricity mixes of N0-f and N0-fb in 2040 and 2050 present a noticeably higher share in wind production. In N0-f the transition from 2030 to 2050 is smoother than the one in N0-fB scenario. In fact, in the latter, the model is incentivized to install more renewable capacity to decarbonize the power sector, since it is harder to reduce the emission of the upstream sector in case of limited access to biomass. The need of electricity to feed electrolysis hydrogen production is also visible from the increase in the total electricity demand from scenario N0-f to scenario N0-fB.

As in the case of BAU scenario, differences between the electricity mix of N0 and N0-B scenarios are negligible, except for a slight increase in the total electricity demand in 2040 and 2050 to permit hydrogen production from electrolysis.

For C scenario, differences between its electricity mix and the one of N0 are negligible. The same happens between C-f and N0-f results. Apart from a negligible decrease in the thermoelectric generation compensated by a small growth of solar electricity and of import, no significant difference is observed. Indeed, the main differences between these two pair of scenarios are in the upstream sector and will be tackled in Section 3.2.

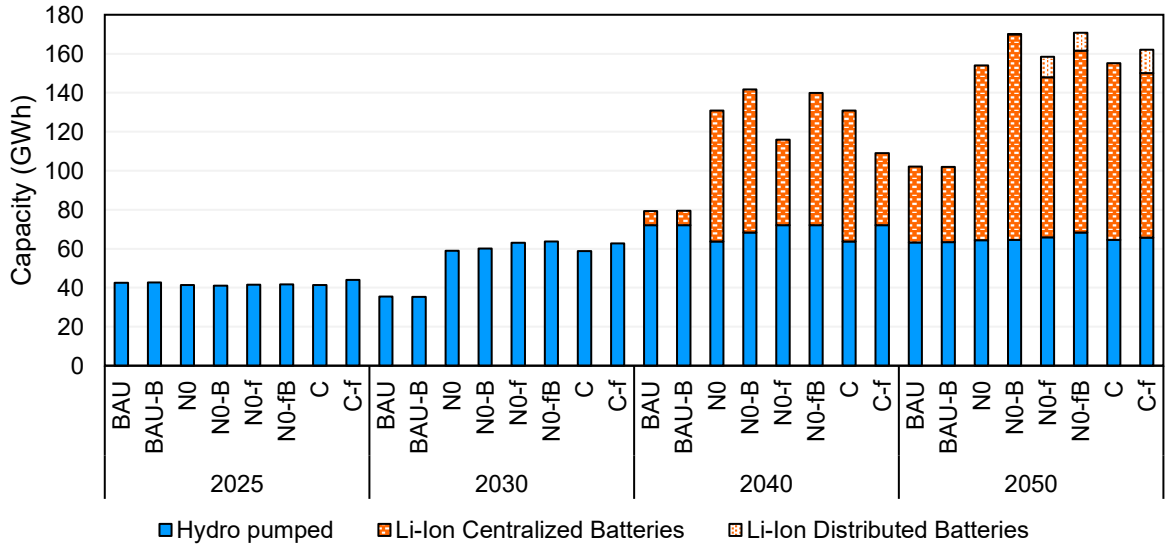

Figure 22. Storage capacity by technology kind in the different scenarios.

Storage capacity throughout the analysed period in the different scenarios is presented in Figure 22. Two of the three groups of storage technologies are installed from the model: hydroelectric pumped storage and Lithium-Ion batteries. Vanadium-Redox-Flow batteries are not considered optimal in any scenario indeed, despite their specific investment cost becomes lower than the one of Lithium-Ion batteries from 2040, their lower efficiency and shorter life do not make them a cost-effective option. Regarding Lithium-Ion batteries, the largest fraction is made of centralized batteries, while distributed ones become cost-effective only in 2050 in N0-f, N0-fB and C-f scenarios. Up to 2030, the hydro pumped storage capacity is sufficient to sustain the needs of the Italian energy system. From 2040 on, Li-Ion batteries are installed in all scenarios. Concurrently, introducing an emission limit, the storage needs of the system significantly increase due to a higher renewable penetration in the technology mix.

The regional distribution of solar and wind capacity deployed is reported in Table 17 and Table 18, respectively. Table 17 shows that the solar source is distributed throughout Italy. In most regions, from 2025 to 2050 the installed capacity grows. However, the largest shares of the capacity in 2050 are concentrated in high demand regions like Emilia Romagna and Lombardia and in resourceful ones like Puglia and Sicilia.

By observing the wind capacity in Table 18, the asymmetry of wind resource and of its distribution throughout Italy is highlighted. In fact, southern regions like Campania, Puglia, Sardegna and Sicilia present significantly high wind installed capacities in all the decarbonization scenarios, while most other regions show installed capacities lower than 1 GW. Moreover, it is interesting to observe the regional differences between solar and wind installed capacity between scenarios presenting negligible differences regarding their energy mix. The equilibrium point of the model regarding the share of the electricity generated by variable renewable resources at Italian level appears to be quite stable, while regional differences appear to be driven by the cost-optimization function.

For BAU, N0 and N0-f scenarios, the photovoltaic, wind and storage capacity across the regions are represented in Figure 23. In the northern regions, the installed capacities for these three categories do not vary significantly across the scenarios, except in the case of Emilia-Romagna. This region has the highest resource availability in the North due to the assumed capacity factors and is therefore selected as the optimal location for renewable generation – particularly solar – in the decarbonization scenarios. In the southern regions, Campania, Puglia, and Sicily show the largest increases in both renewable and storage capacities, with the largest share of installation being in wind capacity.

Table 17. Regional solar capacity (GW) in 2025 and 2050 in the different scenarios.

	BAU		BAU-B		N0		N0-B		N0-f		N0-fB		C		C-f	
	2025	**2050**	**2025**	**2050**	**2025**	**2050**	**2025**	**2050**	**2025**	**2050**	**2025**	**2050**	**2025**	**2050**	**2025**	**2050**
ABR	1.87	2.39	1.87	2.47	1.88	0.72	1.85	0.74	1.87	0.85	1.87	0.88	1.88	0.71	1.87	0.76
BAS	0.42	0.35	0.42	0.35	0.43	0.98	0.43	0.98	0.43	0.99	0.43	0.98	0.43	0.98	0.43	0.98
CAL	0.69	0.96	0.69	0.96	0.73	0.71	0.74	0.61	0.71	0.45	0.71	0.73	0.73	0.71	0.71	0.61
CAM	2.50	2.99	2.50	2.99	2.50	2.44	2.50	2.90	2.50	8.51	2.50	8.51	2.50	2.50	2.50	8.49
EMR	3.88	20.02	3.83	19.81	2.98	32.45	2.87	37.17	2.63	7.18	2.63	12.08	3.02	32.32	2.63	7.32
FVG	0.42	1.21	0.44	1.20	0.26	2.09	0.26	2.01	0.26	2.68	0.26	2.54	0.26	2.07	0.26	2.68
LAZ	2.26	4.49	2.26	4.51	2.12	7.17	2.18	7.35	2.26	7.53	2.26	7.56	2.11	7.11	2.26	7.51
LIG	0.68	1.24	0.68	1.24	0.67	1.88	0.67	1.82	0.67	2.41	0.67	2.44	0.67	1.88	0.67	2.41
LOM	3.10	9.28	3.09	9.29	3.64	12.91	3.64	12.74	3.60	16.32	3.57	16.28	3.63	12.91	3.61	16.23
MAR	1.40	0.53	1.40	0.53	1.42	1.48	1.42	1.48	1.43	1.09	1.43	1.13	1.42	1.49	1.43	1.06
MOL	0.20	0.23	0.20	0.23	0.21	0.14	0.21	0.15	0.21	0.11	0.21	0.09	0.21	0.14	0.21	0.18
PIE	2.42	7.55	2.41	7.67	3.99	8.87	3.95	8.74	4.00	3.96	3.99	5.76	3.96	9.51	4.08	4.33
PUG	4.41	4.86	4.41	4.86	4.49	13.94	4.49	13.96	4.49	14.12	4.49	14.07	4.49	13.94	4.49	14.09
SAR	2.29	2.25	2.29	2.26	2.32	6.50	2.31	6.53	2.32	6.66	2.33	6.64	2.32	6.49	2.33	6.65
SIC	4.62	4.09	4.63	4.10	4.61	6.92	4.61	9.29	4.68	11.56	4.68	12.43	4.61	6.93	4.63	11.97
TAA	0.21	1.47	0.21	1.47	0.21	1.64	0.21	2.82	0.21	0.80	0.21	1.14	0.21	1.73	0.21	0.87
TOS	2.71	2.43	2.71	2.43	2.68	2.45	2.59	2.19	2.81	3.02	2.83	3.02	2.66	2.39	2.78	3.02
UMB	0.22	0.38	0.22	0.39	0.22	1.04	0.22	1.00	0.22	1.01	0.22	0.84	0.22	1.03	0.22	1.19
VDA	0.01	0.00	0.01	0.00	0.01	0.03	0.01	0.05	0.01	0.00	0.01	0.01	0.01	0.03	0.01	0.00
VEN	1.97	3.68	1.96	3.68	2.68	3.84	2.91	3.74	2.89	3.41	2.87	3.60	2.69	4.22	2.77	3.25
Total	10.4	48.1	10.4	48.2	10.8	56.3	10.8	60.7	10.7	111.9	10.7	111.9	10.8	56.3	11.12	111.9

Table 18. Regional wind capacity (GW) in 2025 and 2050 in the different scenarios.

	BAU		BAU-B		N0		N0-B		N0-f		N0-fB		C		C-f	
	2025	**2050**	**2025**	**2050**	**2025**	**2050**	**2025**	**2050**	**2025**	**2050**	**2025**	**2050**	**2025**	**2050**	**2025**	**2050**
ABR	0.27	2.58	0.27	2.66	0.27	0.24	0.27	0.24	0.27	0.89	0.27	0.76	0.27	0.23	0.27	0.79
BAS	0.70	1.93	0.70	1.93	0.70	5.29	0.71	5.26	0.71	5.41	0.71	5.36	0.70	5.30	0.71	5.38
CAL	0.78	4.50	0.78	4.50	0.85	0.95	0.85	0.83	0.81	1.60	0.81	1.27	0.85	0.95	0.79	1.16
CAM	1.87	11.76	1.87	11.75	1.87	5.32	1.87	7.93	1.87	33.48	1.87	33.17	1.87	5.23	1.87	33.36
EMR	0.07	0.60	0.07	0.60	0.05	0.66	0.05	0.75	0.05	0.60	0.05	0.60	0.05	0.66	0.05	0.60
FVG	0.00	0.11	0.00	0.11	0.00	0.18	0.02	0.17	0.00	0.24	0.00	0.22	0.00	0.18	0.00	0.24
LAZ	0.08	0.63	0.08	0.63	0.08	0.00	0.08	0.00	0.08	1.05	0.08	1.01	0.08	0.00	0.08	1.04
LIG	0.05	0.12	0.05	0.12	0.05	0.17	0.05	0.17	0.05	0.22	0.05	0.23	0.05	0.17	0.05	0.22
LOM	0.00	0.83	0.00	0.84	0.00	1.15	0.00	1.13	0.00	1.48	0.00	1.44	0.00	1.15	0.31	1.47
MAR	0.02	0.08	0.02	0.07	0.02	0.00	0.02	0.00	0.02	0.00	0.02	0.00	0.02	0.00	0.02	0.00
MOL	0.40	0.90	0.40	0.90	0.40	0.17	0.40	0.17	0.40	0.43	0.40	0.30	0.40	0.17	0.40	0.71
PIE	0.02	0.68	0.02	0.69	0.27	0.79	0.13	0.79	0.06	0.36	0.11	0.51	0.27	0.85	0.28	0.40
PUG	2.81	8.74	2.81	8.73	2.85	23.35	2.90	23.34	2.91	25.36	2.90	24.72	2.85	23.34	2.79	25.04
SAR	1.09	4.09	1.09	4.10	1.09	11.57	1.09	11.61	1.09	12.46	1.09	12.18	1.09	11.56	1.09	12.29
SIC	2.12	9.45	2.12	9.48	2.12	5.33	2.12	7.16	2.12	27.11	2.12	28.89	2.12	5.35	2.12	28.01
TAA	0.00	0.13	0.00	0.13	0.00	0.14	0.02	0.24	0.02	0.07	0.00	0.09	0.00	0.14	0.02	0.07
TOS	0.14	0.64	0.14	0.64	0.14	0.65	0.14	0.58	0.14	0.79	0.14	0.79	0.14	0.63	0.14	0.79
UMB	0.00	0.00	0.00	0.00	0.00	0.00	0.00	0.00	0.00	0.00	0.00	0.00	0.00	0.00	0.00	0.00
VDA	0.00	0.00	0.00	0.00	0.00	0.00	0.00	0.00	0.00	0.00	0.00	0.00	0.00	0.00	0.00	0.00
VEN	0.01	0.35	0.01	0.35	0.02	0.35	0.06	0.34	0.10	0.33	0.05	0.34	0.02	0.38	0.15	0.31
Total	36.3	70.4	36.3	70.4	38.1	108.2	38.1	116.3	38.2	92.6	38.2	100.8	38.1	109.1	38.1	93.6

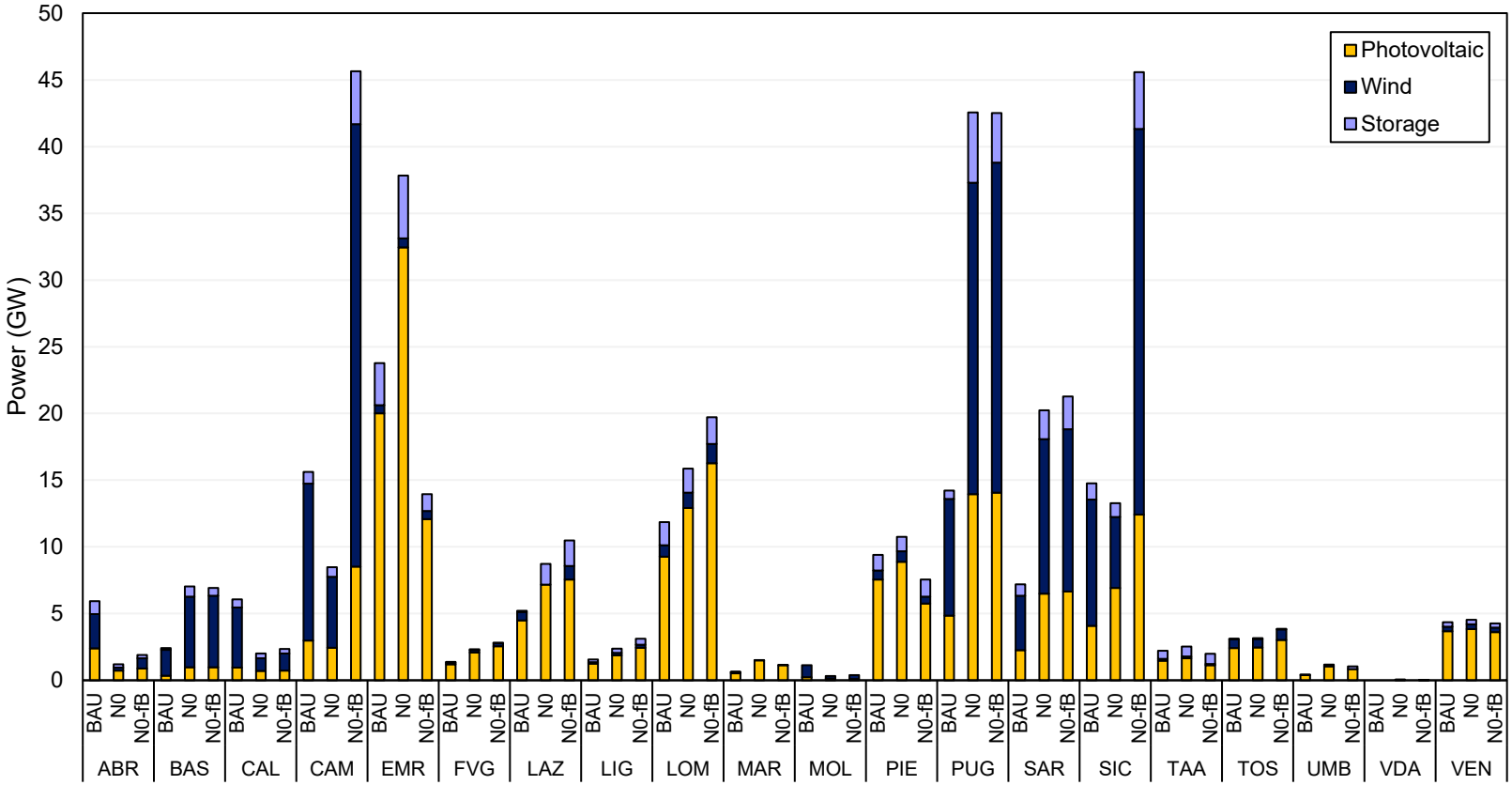

Figure 23. Regional distribution of photovoltaic, wind and storage capacity in 2050 in scenarios BAU (a), N0 (b) and N0-fB (c).

To analyse the scenario results it is also useful to observe the electricity generation profiles for some scenarios. Comparing Figure 24b and Figure 25 the first difference consists of the load profiles: in N0 and N0-fB the electricity load is increased by around 10 GW due to a larger electrification in the technologies of transport and residential sectors. Regarding load, the slight increase between 11:00 and 13:00 for scenario N0-fB is due to hydrogen production from electrolysis and is consequently absent in N0 scenario (see Section 3.2). This also causes the difference between the two storage charging shapes. Moreover, from N0 to N0-fB a part of thermoelectric generation and solar generation is substituted by wind generation. Import as well decreases from N0 to N0-fB scenario. The electricity generation profile significantly changes even in BAU scenario: the thermoelectric input is halved and substituted by storage systems – charged by an increased solar generation – and by import.

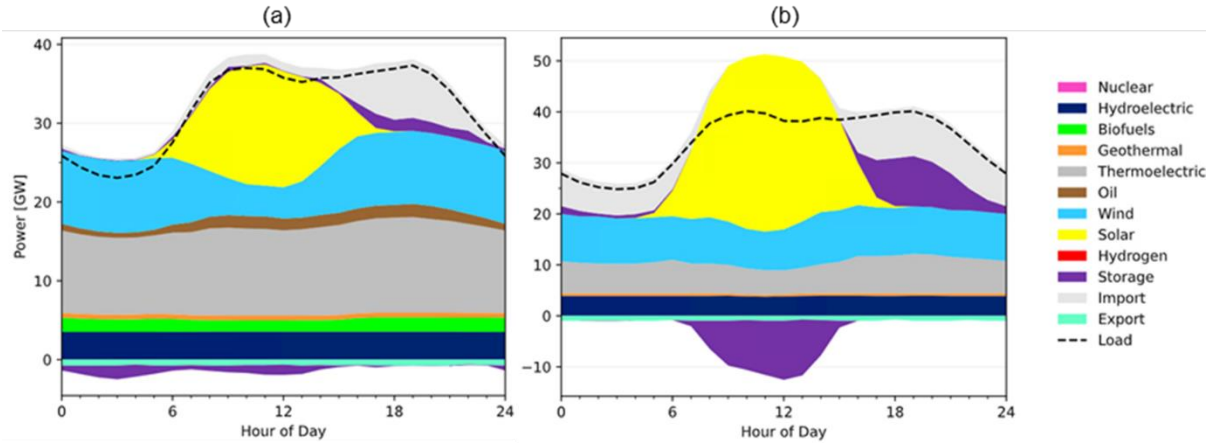

Figure 24. Italian electricity load and generation profile in 2025 (a) and 2050 (b) for BAU scenario.

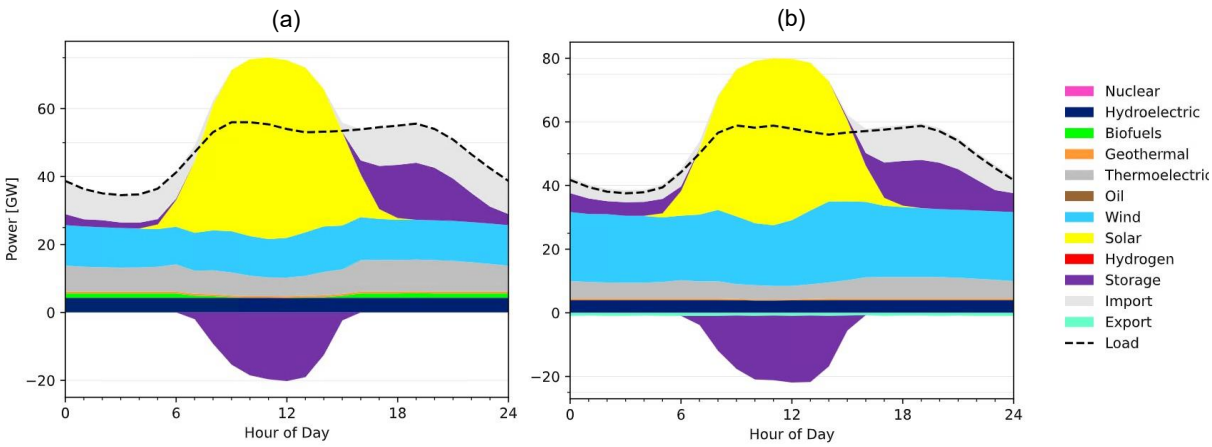

Figure 25. Italian electricity load and generation profile in 2050 for N0 (a) and N0-fB (b) scenarios.

About electricity transmission, Figure 26 shows the results of scenarios BAU, N0, N0-f and N0-fB. The transmission capacity resulting from the model scenarios from 2025 to 2050 is compared to the existing transmission capacities in 2022 (taken from Terna statistics [78]). As for the electricity mix, the results regarding transmission capacity for BAU scenario is the same of BAU-B one. The same happens for N0, N0-B and C and for N0-f and C-f.

Lacking emission reduction targets, transmission capacity reaches values close to Terna ones, as results of BAU scenario show. The comparison between BAU and N0 scenario shows that when emission reduction targets are introduced, transmission capacity from Central-Southern Italy towards Central-Northern Italy, the South and Sardegna increases. In N0-f and N0-fB scenarios the transmission capacity strongly increases in 2040 and 2050. Northern and Southern Italy become more interconnected and exploit the higher renewable resource of the South to cover the higher demand of Northern Italy.

Specifically, in N0-fB scenario the transmission capacity increase is the most gradual, despite reaching transmission values similar to the N0 ones in 2050. The transmission distance of N0-fB is slightly lower in some lines compared to the one of N0, since part of the electricity is used locally for hydrogen production via electrolysis.

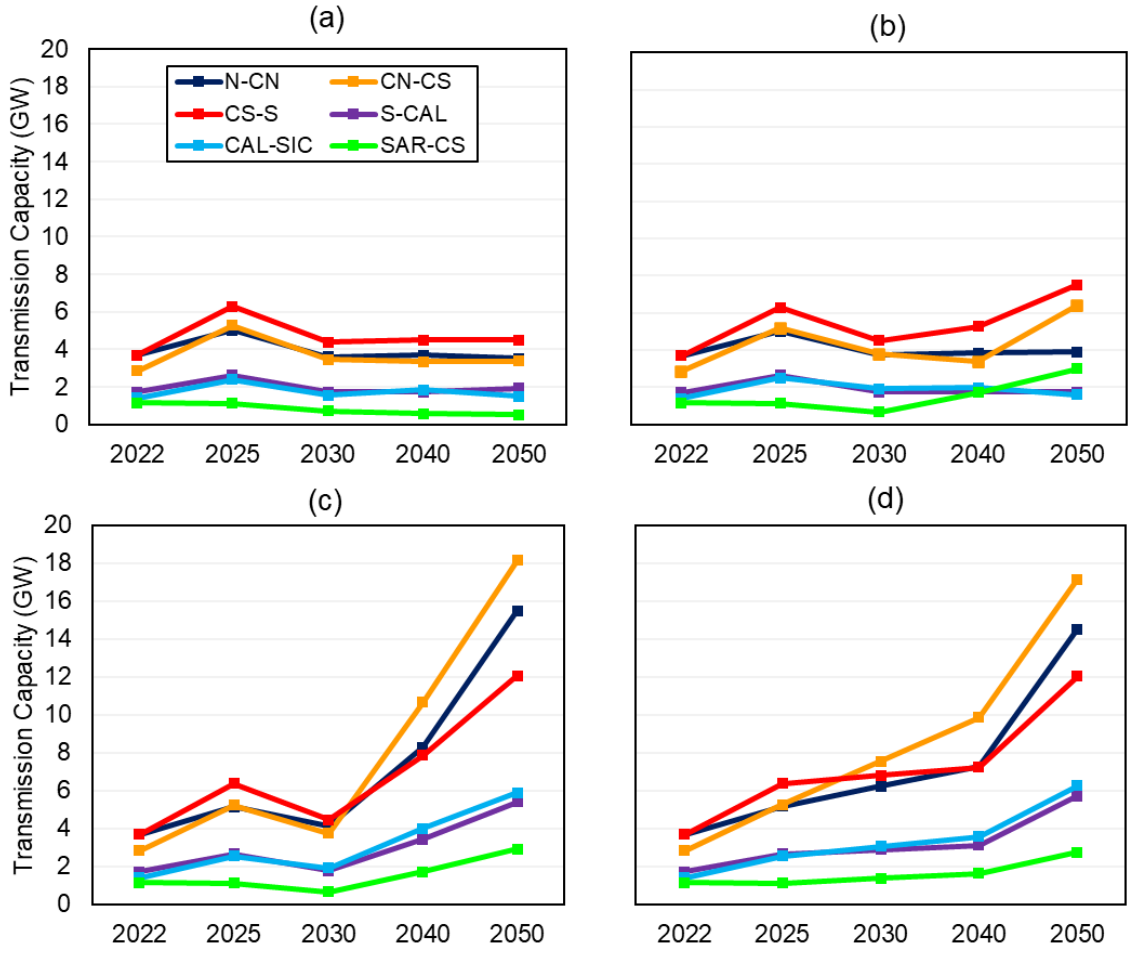

Figure 26. Electric transmission capacity between bidding zones for BAU (a), N0 (b), N0-f (c) and N0-fB scenarios from 2025 to 2050 compared to Terna's values for 2022 [78].

3.2 Hydrogen production and consumption

Another relevant aspect in the scenario analysis results is hydrogen production. The evolution of the hydrogen production mix is shown in Figure 27. As is highlighted in Figure 27, the hydrogen sector is hard to decarbonize. By observing the results for BAU, N0, N0-F, C and C-F scenarios, biomass steam reforming appears to be the cheapest hydrogen production process from 2025 to 2050. However, from 2040 on a small share of electrolysis enters the hydrogen production mix in some scenarios meaning that increasing the cost of natural gas and decreasing the CO_2 emission limit makes the two technologies compete. In C and C-f scenarios, to reach the negative emission limits discussed in Section 2.2, the model needs to install biomass gasification plants with carbon capture for hydrogen production.

The most interesting scenarios to observe are N0-B and N0-fB. Due to the constraints imposed on hydrogen production from biomass and the high cost of electrolysis, up to 2030 the main hydrogen production method is steam reforming of natural gas. In 2040, emission limits become stronger and hydrogen demand grows, so new hydrogen production installations mainly consist of natural gas steam

reforming facilities with CCS and of electrolysis ones. Finally, in 2050 hydrogen production from natural gas steam reforming without CCS is completely substituted by electrolysis.

The difference between the hydrogen production level in the different scenarios depends on hydrogen cost, which influences the cost-effectiveness of different hydrogen uses. For simplicity, in Figure 28 only scenarios N0-f, N0-fB and C-f are compared.

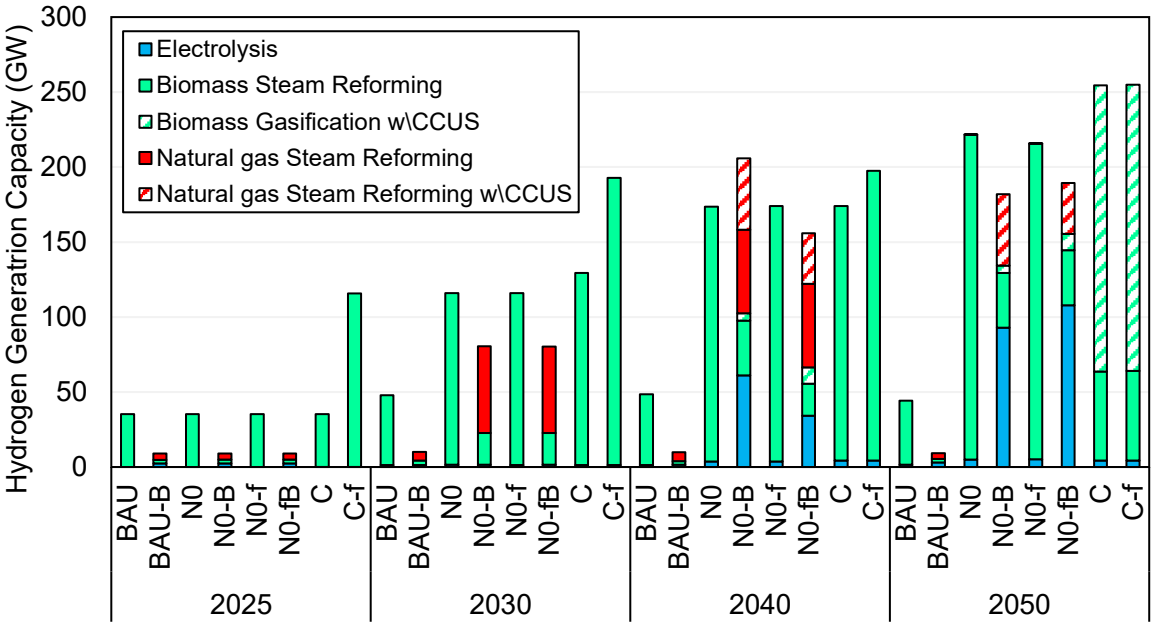

Figure 27. Hydrogen production processes in the different scenarios in the modeled period.

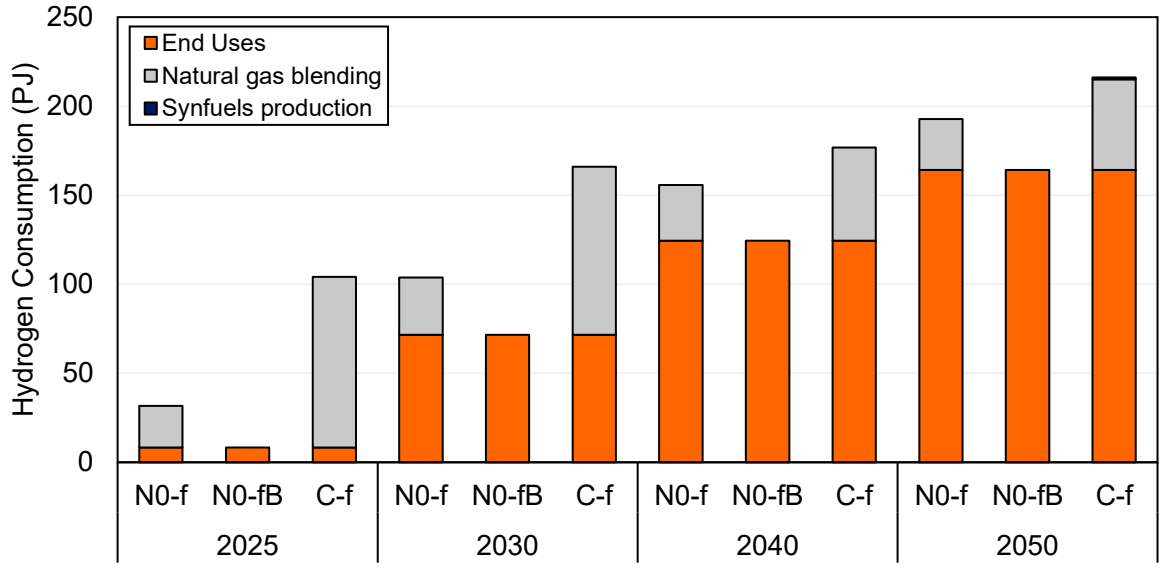

Figure 28. Hydrogen consumption by use in N0-f, N0-fB and C-f scenarios.

From Figure 28 is evident that the hydrogen demand level for end uses is equal for the three scenarios in the same year. However, the total demand varies, mostly due to the quantity of hydrogen blended in natural gas pipelines. When hydrogen is produced by biomass gasification, blending with methane is a cost-effective solution to decrease the carbon content of natural gas. The production of synthetic fuels is not selected from the model except for a small fraction in scenario C-f in 2050 because of its high cost.

3.3 Investigation of the cost conditions for the SCEP competitiveness

In this Section of the work one of the scenarios presented in Section 2.2 is selected to perform the sensitivity analysis introduced in Section 2.3. The scenario choice is made by considering the results of the scenario analysis in Section 3.1. The scenario used to investigate the cost-competitiveness of SCEP should be characterized by:

a. the presence of an **emission limit**, making it compliant with emission reduction targets from the European Union;
b. an **increasing transmission capacity** from 2022 to 2050, to investigate the possible role of SCEP in substituting capacity additions of traditional lines;
c. **diversified hydrogen production** mix: in the case of hydrogen fully produced by biomass, there would be no significant advantage in a hydrogen transmission system since all regions could easily sustain their own demand.

For these reasons, scenario N0-fB is chosen for evaluating the SCEP potential role in the Italian energy system.

In Figure 29 the 2050 electricity transmission capacity previously resulting by the N0-fB scenario is reported.

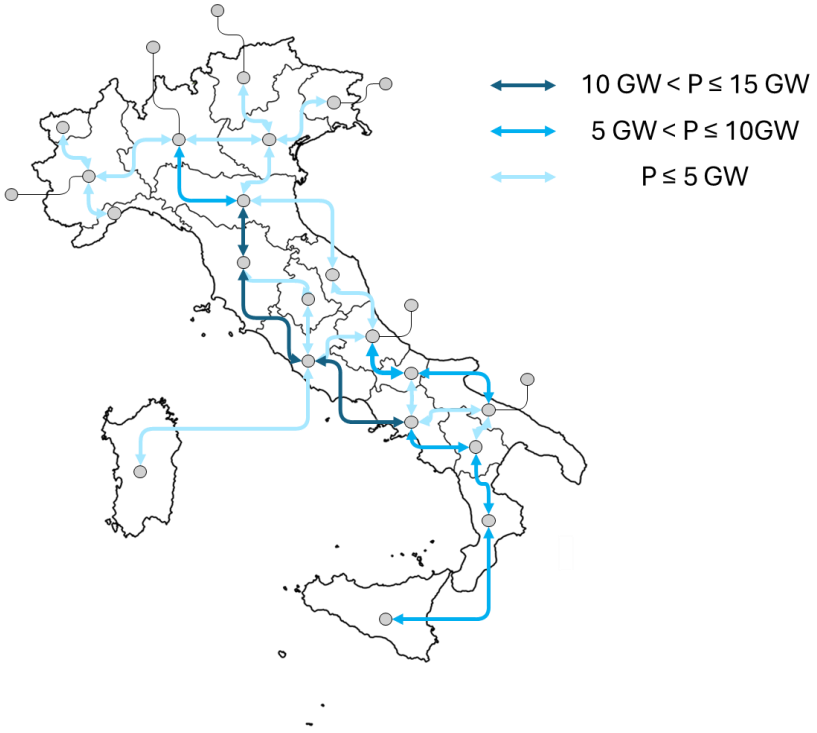

Figure 29. Regional electricity transmission lines in 2050 for the N0-fB scenario.

By observing Figure 29, the connections with the highest installed power in 2050 are the ones favouring electricity transmission from Southern Italy towards Emilia Romagna and Lombardia. The installation of SCEP is expected on the highest power lines, favouring it a more efficient electricity transmission.

The first result of the evaluation of SCEP cost-effectiveness throughout the sensitivity analysis scenarios is presented in Figure 30. The graph shows the transmission capacity of SCEP as a function of its investment cost, expressed as a percentage of the baseline, for the three groups of scenarios regarding the cost of conventional transmission. The transmission capacity is expressed in GW*km to include the transmission distance of the lines in the results presented losing their dependence on the

starting assumption of transmission distances. As the investment cost of SCEP decreases, the specific installed capacity increases sharply, particularly when the cost of traditional electricity transmission is high. As the cost of traditional electricity transmission increases, the curve shifts upward and to the right. The cost of metallic materials composing the traditional lines is identified as an important parameter influencing SCEP diffusion. Therefore, SCEP would be an interesting solution for energy transmission in scenarios considering geopolitical risks as a factor influencing the cost of primary commodities.

This trend highlights the importance of the cost of conventional electricity transmission infrastructure – and especially of metallic materials – as a key driver for the adoption of SCEP. Therefore, SCEP emerges as a promising solution for energy transmission in scenarios where geopolitical risks lead to increased prices of primary materials.

To better understand the relation between SCEP and conventional transmission, Figure 31 and Figure 32 portray respectively the installed power and the investment cost of transmission by technology kind in the sensitivity scenarios.

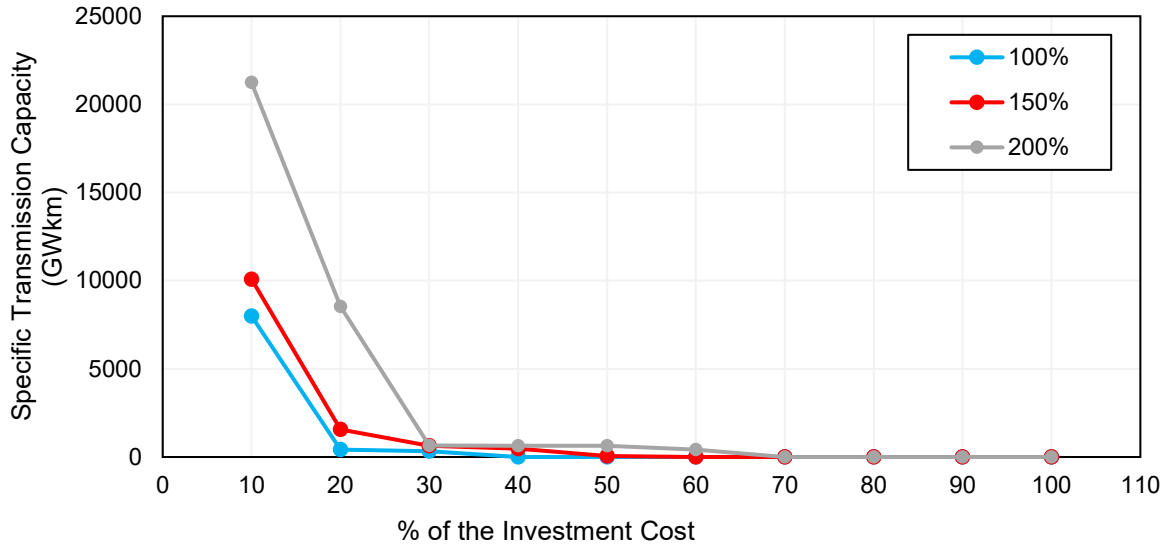

Figure 30. SCEP installed power in 2050 in the three cost scenarios for electricity transmission.

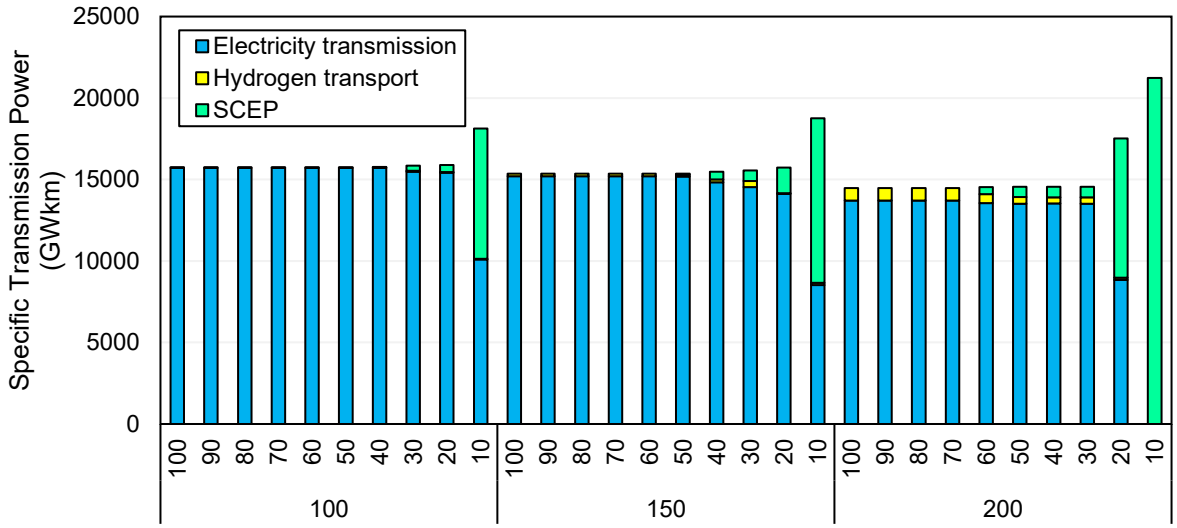

Figure 31. Specific transmission capacity in the sensitivity scenarios in 2050 by technology kind.

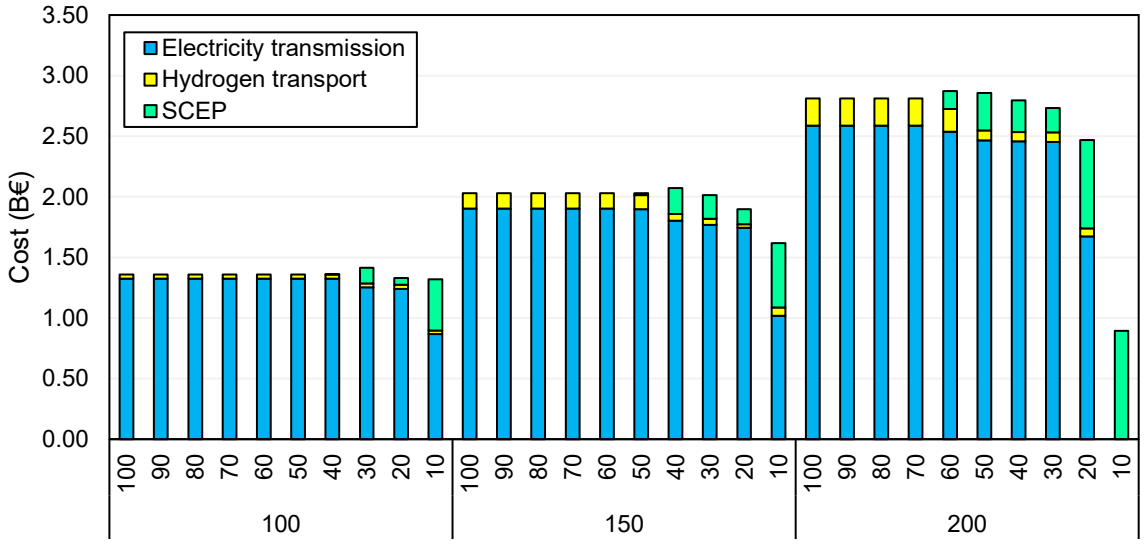

Figure 32. Discounted investment cost for transmission in the modeled period by technology kind across the sensitivity scenarios.

As Figure 31 and Figure 32 highlight, traditional electricity transmission is the preferred transmission path for the model. Both hydrogen transport and SCEP cost effectiveness increases with the cost of electricity transmission. Concurrently, with the introduction of SCEP the investment cost for transmission slightly decreases.

The effect of the two cost variations on the installed capacity of the technology is investigated in Figure 33 and Figure 34 observing the diffusion of the technology in the different transmission lines. The SCEP installed power in the different lines and the direction of electricity and hydrogen flows for different sensitivity scenarios are compared. Specifically, Figure 33 highlights the differences between three scenarios with unchanged cost of electricity transmission but where SCEP cost varies between the 30% and the 10% of the initial cost estimate.

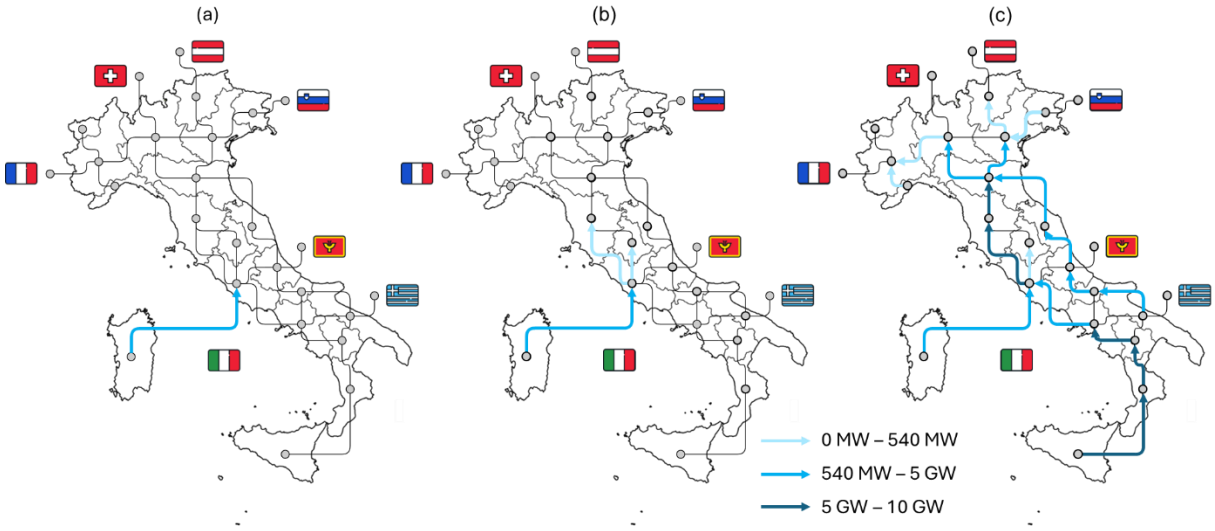

Figure 33. Direction of electricity and hydrogen flows through SCEP in 2050 for scenarios SCEP30_TR100 (a), SCEP20_TR100 (b) and SCEP10_TR100 (c).

As Figure 33 shows, the cost decrease of SCEP has a strong influence not only on the installed power but also on the spatial diffusion of the technology. The cost decrease favours the formation of

two parallel transmission backbones transporting electricity and hydrogen from Sicilia and from Puglia towards Emilia Romagna, where the commodities are split among the Northern regions.

Concurrently Figure 34 shows the influence of the cost of traditional electricity transmission on SCEP installed lines across Italy. Here are compared three scenarios with the same cost reduction for SCEP – with the final cost being 20% of the initial estimate – and with the three considered cases concerning the cost increase of traditional electricity transmission (unvaried, +50% and +100%).

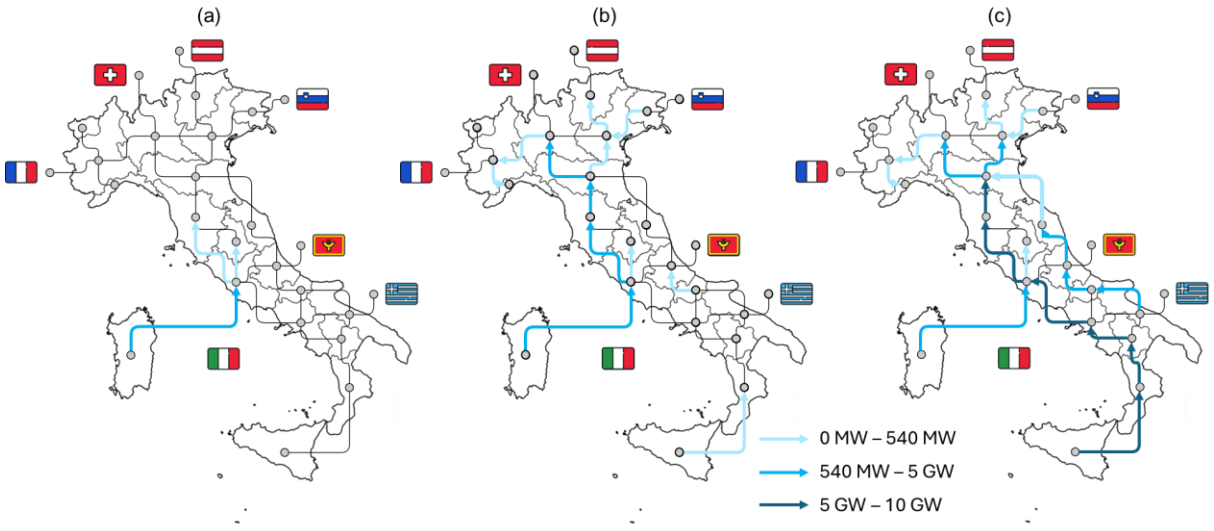

Figure 34. Direction of electricity and hydrogen flows through SCEP in 2050 for scenarios SCEP20_TR100 (a), SCEP20_TR150 (b) and SCEP20_TR200 (c).

By observing Figure 34, the influence of the electricity transmission cost on SCEP diffusion is still high. However, it appears that this cost variation has a stronger impact on the installed power for each line than on the diffusion of the technology per se.

Despite what emerges from the previous analyses, the cost-competitiveness of SCEP does not necessarily imply widespread deployment across Italy. This technology could prove competitive even if installed on a single transmission line, provided the electric power exceeds 300 MW and considered the electricity and hydrogen transport shares described in Section 2.1.4.4.

The level of detail of the model allows to look at the capacity of each transmission line, enabling the identification of cost thresholds at which SCEP becomes a viable option. The overall results of the sensitivity analysis concerning the SCEP installed capacity for each line are summarised in Table 19. SCEP is considered a cost-effective alternative to traditional energy transmission on lines where its total transmitted power exceeds 540 MW– considering 300 MW of electric power and 240 MW of equivalent hydrogen power as from Section 2.1.4.4.

Based on these findings, SCEP becomes cost-effective when its investment cost is reduced to 30% of the baseline under current electricity transmission costs. If electricity transmission costs increase by 50% and 100%, SCEP becomes competitive when its cost is reduced to 40% and 60% of the baseline, respectively. The first line where SCEP is installed in all three scenarios of increased electricity transmission costs is the connection between Sardegna and Lazio.

Table 19. Installed SCEP power (GW) in the different lines in the sensitivity scenarios. In boulder are highlighted the lines with a capacity larger than 540 MW.

Interconnected regions		TR100			TR150					TR200					
		30	20	10	50	40	30	20	10	60	50	40	30	20	10
ABR	LAZ														0.1
ABR	MAR			**0.9**					**2.0**					**0.8**	**5.3**
ABR	MOL			**1.1**				0.1	**2.2**					**1.0**	**6.3**
BAS	CAL			**5.5**					**5.9**					**5.5**	**7.7**
BAS	CAM			**5.7**					**6.8**					**6.3**	**9.1**
BAS	PUG														0.2
CAL	SIC			**5.6**				0.2	**6.1**					**6.3**	**8.4**
CAM	LAZ			**4.9**					**6.0**					**5.4**	**17.6**
CAM	MOL														0.2
CAM	PUG														0.1
EMR	LOM			**3.4**				**1.2**	**4.5**					**3.3**	**11.0**
EMR	MAR			**0.7**					**1.7**					0.5	**4.4**
EMR	TOS			**5.6**				**1.4**	**6.4**					**6.1**	**14.8**
EMR	VEN			**1.5**				0.2	**2.2**					**1.8**	**6.2**
FVG	VEN			0.1				0.1						0.2	1.1
LAZ	SAR	**1.6**	**1.9**	**3.5**	0.3	**2.3**	**3.2**	**3.3**	**4.3**	**2.1**	**3.2**	**3.2**	**3.3**	**4.2**	**3.9**
LAZ	TOS		0.1	**6.7**				**1.6**	**7.4**					**7.1**	**17.5**
LAZ	UMB		0.1	0.1				0.1	0.2					0.2	**0.9**
LIG	PIE			0.2				0.2	0.4					0.1	**0.8**
LOM	PIE			0.4				0.4	**0.9**					0.4	**2.3**
MOL	PUG			**1.0**					**2.2**					**0.9**	**6.4**
PIE	VDA								0.1						0.5
TAA	VEN			0.1				0.1	0.5					0.1	**1.4**
TOS	UMB														0.1

From the assessment made, the connection between Sardegna and Lazio is the line where the most significant changes occur regarding SCEP installation. For this reason, the yearly electricity generation profile of Sardegna is obtained both for the SCEP100_TR100 and SCEP20_TR100 scenarios. The introduction of SCEP on the line connecting Sardegna and Lazio does not impact on the generation mix of the region, as is observed in the positive quadrant of Figure 35a1 and Figure 35b1. However, observing the negative quadrant of the same figures, there is a small variation in the stored and exported power while introducing SCEP, since the electricity load in Figure 35b1 increases with respect to Figure 35a1. The largest difference between the electricity load in the two scenarios is furtherly highlighted in Figure 35a2 and Figure 35b2 and consists of the strong increase in the electricity needed for hydrogen production from electrolysis.

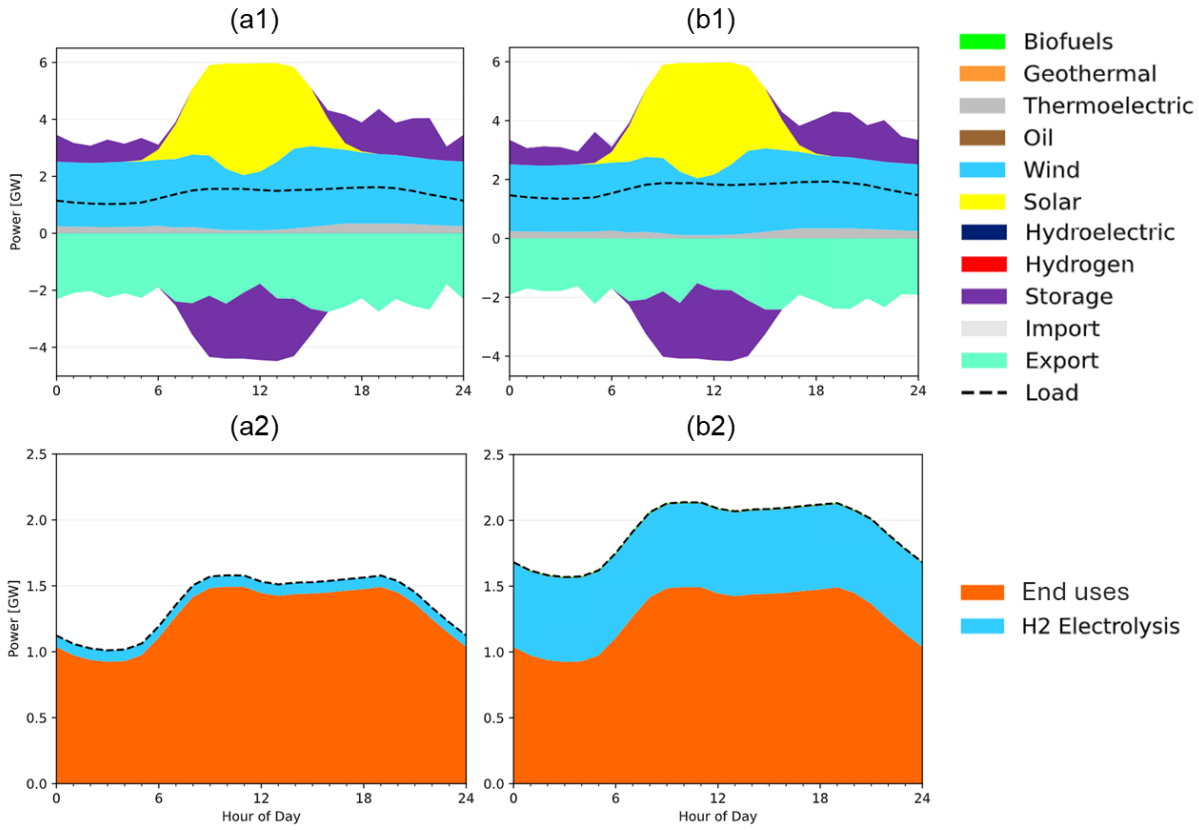

Figure 35. Electricity generation profiles (1) and load composition (2) for Sardegna in 2050 for scenarios SCEP100_TR100 (a) and SCEP20_TR100 (b).

Concurrently, the hydrogen production mix for these two scenarios is analysed for regions which are impacted from SCEP installation. Specifically, it is analysed the behaviour of the regions which interconnection results significant both from the electric power perspective (see Figure 29) and from SCEP capacity one (see Figure 30 and Figure 31) in scenario SCEP20_TR100: Sardegna, Lazio, Toscana and Emilia Romagna. In the SCEP100_TR100 scenario where SCEP capacity is null – as from Figure 36a – all region are self sufficient regarding hydrogen production. The electricity mix of each of them is mainly based on biomass steam reforming and on hydrogen electrolysis. Nevertheless, in scenario SCEP100_TR100 (Figure 36b) the installed capacity of electrolysis plants to produce hydrogen in Sardegna increases: most of the hydrogen produced in the region is exported in Lazio through SCEP. The installation of SCEP favours the centralization of the hydrogen production increasing the production efficiency and favouring the installation of plants in zones with higher renewable production.

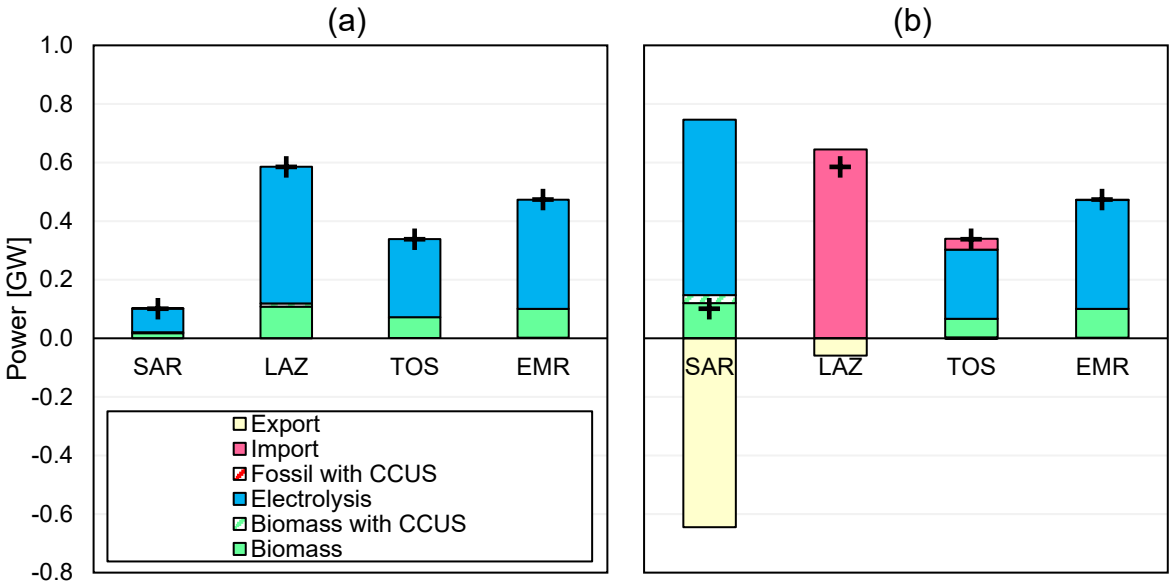

Figure 36. Hydrogen demand and production mix in 2050 in Sardegna for SCEP100_TR100 (a) and SCEP20_TR100 (b) scenarios. The data is expressed in equivalent hydrogen power.

Chapter 4

Conclusions, limitations and perspectives

This thesis assessed the potential role of SCEP technology as an alternative to conventional transmission technologies in the Italian energy system. A multi-regional model instance of the Italian power and hydrogen sectors was developed to analyse the techno-economic viability of SCEP and to identify cost thresholds under which its installation is expected to be cost-effective.

The main methodological innovation of this work lies in the spatial resolution of the model. Indeed, a multi-regional representation of the Italian energy system becomes essential when the focus is on transmission technologies. The implemented model was used to formulate scenarios concerning transmission capacity expansion, the evolution of electricity and hydrogen production mixes and storage requirements. The spatial disaggregation of the model allowed results to be analysed both at national and regional levels, enabling a more accurate characterization of resource availability and demand in each region.

The results of the analysis indicate that, while SCEP is not universally competitive under current cost assumptions, it becomes a cost-effective solution under specific conditions – specifically in emission reduction scenarios where an increase in cross-regional transmission capacity is needed – for decreased investment costs of SCEP. In the scenario analysed, and assuming current cost conditions for conventional electricity transmission, SCEP must reach 30% of its baseline cost to be installed by the system. The identified cost-reduction necessary for SCEP to become viable reduces when costs for metallic materials used in conventional electricity transmission technologies rise. Specifically, if the cost of conventional electricity transmission increases by 50%, SCEP becomes viable at 40% of its baseline cost. If conventional transmission costs double (i.e., increase by 100%), SCEP becomes viable at 60% of its baseline cost. Another aspect verified by the model is that the first lines where SCEP installation is becomes cost-effective are submarine lines, making it compliant with the initial purpose of the project: to use it to connect offshore plants with the mainland. SCEP installation favours the centralization of hydrogen production plants – mainly of electrolysis ones – in regions of high resource availability of renewables.

Several limitations in the proposed study should be acknowledged. First, the implementation of bottom-up energy models requires reliable data both for technology description and for demand and resource input. Such data are not always complete or available, especially at regional level, requiring the introduction of assumptions in the model development. From a spatial and temporal perspective, the regional disaggregation of the model and the time step used represents an improvement over the original TEMOA-Italy structure. However, achieving greater spatial and temporal resolution comes at the expense of the integrated nature of the TEMOA-Italy model, as it was necessary to limit complexity to avoid excessively high computational costs. Another model simplification resides in the representation of renewable resources, a typical feature of fully-integrated multi-sectorial ESOMs: average capacity factors trends cannot capture their inherent intermittency. An increase in the number of time-steps or typical days considered improves the description of resource variability, while actual intermittency can only be captured by PSOMs. For these reasons, the results of this work are not intended to serve as a reference for detailed grid or storage sizing, but rather as a benchmark to evaluate the effects of different constraints on the transmission system. Lastly, being the techno-economic characterization of SCEP still in an early research phase, its techno-economic parameters remain uncertain and may evolve as the technology matures. SCEP model characterization is based on current literature and preliminary design studies, which may not capture the full range of technical challenges and costs inherent in its operation, and for that it is an intrinsic limitation of the model.

Further methodological research is needed to assess whether the advantages of a multi-regional model are limited to the representation of transmission capacity expansion or if other significant benefits can be identified and quantified. Regarding SCEP economic feasibility study, future work could include a parametric analysis to evaluate how hydrogen mass flowrate in the pipeline could influence the cost-effectiveness of the technology.

To conclude, although SCEP is still far from being a mature or widely deployable technology, it shows the potential to play a role in an expanding and increasingly diversified transmission system, in alignment with the energy transition goals. This work contributes to the discussion around hybrid infrastructures and their role in enabling the transition to a low-carbon energy system. In particular, it highlights how solutions like SCEP could be relevant in countries like Italy, where regional heterogeneity and need of reliable interconnection systems are fundamental elements for energy system planning.

Acknowledgements

Per diversi mesi, cercando di motivarmi a completare questo percorso pensavo alla laurea e ai ringraziamenti che avrei voluto fare in quel momento alle persone che mi sono state vicine in questo strano periodo. Ora ci sono arrivata, anzi ci siamo, ed esprimermi non è così facile come mi sembrava mesi fa, ma ci voglio comunque provare.

Prima di tutto vorrei ringraziare la professoressa Savoldi per l'opportunità di lavorare su queste tematiche, per essersi mostrata disponibile nei miei confronti e avermi subito dato fiducia, per aver dimostrato la passione e i valori che mette al servizio del suo lavoro di insegnamento e di ricerca. Vorrei ringraziare anche Matteo per il suo continuo appoggio durante il lavoro di tesi e per essersi confrontato con me sul mio futuro, per i suoi consigli sempre utili e per avermi trasmesso l'entusiasmo che si può trovare quando si fa qualcosa che ci appassiona.

Ora un pensiero alla mia famiglia, ai miei genitori che mi hanno dato la possibilità di studiare e mi hanno tenuto la mano durante questo percorso, spingendomi con delicatezza quando necessario e pensando sempre a me e alla mia felicità, ad Agnese che non vedo l'ora di riabbracciare ogni volta che rientra a casa e con cui l'intesa non passa mai, a Pietro che ammiro così tanto per il suo impegno e le sue passioni, a Eme che mi ha mostra tutti i giorni cosa vuol dire cercare di seguire il proprio sogno nonostante tutto, alla mia nonna che sicuramente si emozionerà in cui vedo un entusiasmo nelle cose che a tratti io non riesco ad avere, e al nonno che vuole sempre imparare cose nuove ed essere sempre informato sul mondo. Vi voglio tanto bene e vi ringrazio per essere stati al mio fianco sia nei momenti più felici sia in quelli più bui.

Grazie a Giovanni che mi ha sempre circondata di amore e cura e mi ha sempre spinto a cercare di raggiungere la serenità. Mi hai aiutata a capire cosa voglio e mi hai accompagnata per mano per renderlo possibile quando da sola non riuscivo, e per questo ti sarò sempre grata.

Vorrei poi ringraziare tanto i miei compagni di corso. A Fra con cui dall'aula 4 non ci siamo più mollate, per il sostegno costante e la presenza, le chiacchiere, le risate, i discorsi filosofici e il confrontarci su tutto. Ai miei compagni energetici perché dopo il lockdown ci siamo dati esattamente ciò di cui avevo bisogno in quel momento: leggerezza, libertà, amicizia. Lo ricorderò sempre come uno dei momenti più belli del mio percorso. Grazie anche a chi è arrivato dopo o chi si è fatto conoscere piano piano. Grazie a Tommi per il tuo silenzioso appoggio a Lisbona. Grazie a Lore perché sei stato veramente un amico in questi anni e più di altri sei riuscito a capire certe mie paure riguardo al percorso, e con Sara compagno di studio di fiducia: grazie a voi due ricorderò come positivo lo studio matto e disperatissimo per superare certi scogli. Sono così contenta che siamo riusciti a laurearci insieme. Voi tutti quanti avete reso questo percorso e questa esperienza speciale, mi avete dato qualcosa che cercavo da tempo e anche se dovesse restare tutto legato a questa parentesi non posso che ritenermi soddisfatta di quello che è stato.

Grazie a tutti gli altri miei amici e amiche che mi sono stati accanto in questo percorso, da vicino e da lontano. Grazie ad Ari ed Emma, Sara, Marta, Rebi, Fra, Robi, Ila ed Eli.

L'ultimo pensiero va a tutte le altre persone che ho incontrato al Politecnico, alle amicizie che si sono perse, alle mille cotte sui banchi e nei corridoi, alle persone con cui ho scambiato due parole in pullman o in aula, ai professori che hanno lasciato in me qualcosa e a quelli che non lo hanno fatto. Tutto questo ha lasciato in me qualcosa che mi porta ad essere chi oggi sono, e ne sono grata. Sono così fortunata.

"Canterò le mie canzoni per la strada
ed affronterò la vita a muso duro [...]
con un piede nel passato,
e lo sguardo dritto e aperto nel futuro"

References

[1] P. Hevia-Koch, B. Wanner, and R. Kuwahata, “Electricity Grids and Secure Energy Transitions,” Oct. 2023. Accessed: May 23, 2025. [Online]. Available: https://iea.blob.core.windows.net/assets/ea2ff609-8180-4312-8de9-494bcf21696d/ElectricityGridsandSecureEnergyTransitions.pdf

[2] G. Arcia-Garibaldi, P. Cruz-Romero, and A. Gómez-Expósito, “Future power transmission: Visions, technologies and challenges,” Oct. 01, 2018, *Elsevier Ltd*. doi: 10.1016/j.rser.2018.06.004.

[3] A. Di Bella, F. Canti, M. G. Prina, V. Casalicchio, G. Manzolini, and W. Sparber, “Power system investment optimization to identify carbon neutrality scenarios for Italy,” *Environmental Research: Energy*, vol. 1, no. 3, p. 035001, Sep. 2024, doi: 10.1088/2753-3751/ad5b64.

[4] C. Medina, A. C. Ríos, and G. González, “Transmission Grids to Foster High Penetration of Large-Scale Variable Renewable Energy Sources – A Review of Challenges, Problems, and Solutions,” *International Journal of Renewable Energy Research*, no. Vol12No1, 2022, doi: 10.20508/ijrer.v12i1.12738.g8400.

[5] R. Benato *et al.*, “CALAJOULE: An Italian Research to Lessen Joule Power Losses in Overhead Lines by Means of Innovative Conductors,” *Energies (Basel)*, vol. 12, no. 16, p. 3107, Aug. 2019, doi: 10.3390/en12163107.

[6] N. Shields, S. Ashworth, T. Heidel, K. Thomas, and F. Moriconi, “Overhead Superconducting Power Transmission,” *ELECTRA - CIGRE’s Digital Magazine*, vol. 330, 2023. Accessed: Jun. 27, 2025. [Online]. Available: https://electra.cigre.org/330-october-2023/technology-e2e/overhead-superconducting-power-transmission.html

[7] K. Cole, “Practicality of superconductors in power transmission,” POWER Engineers, Inc. Accessed: Jun. 27, 2025. [Online]. Available: https://wwwpowerengcom.cdn.prismic.io/wwwpowerengcom/Zyky668jQArT0LVc_PracticalityofSuperconductorsinPowerTransmission_Final.pdf

[8] European Commission, “Communication from the Commission | REPowerEU Plan,” Brussels, 2022.

[9] European Commission, *A hydrogen strategy for a climate-neutral Europe*. 2020. Accessed: Jun. 14, 2025. [Online]. Available: https://eur-lex.europa.eu/legal-content/EN/TXT/?uri=CELEX%3A52020DC0301

[10] B. Miao, L. Giordano, and S. H. Chan, “Long-distance renewable hydrogen transmission via cables and pipelines,” *Int J Hydrogen Energy*, vol. 46, no. 36, pp. 18699–18718, May 2021, doi: 10.1016/j.ijhydene.2021.03.067.

[11] A. Patonia, V. Lenivova, R. Poudineh, and C. Nolden, “Hydrogen pipelines vs. HVDC lines: Should we transfer green molecules or electrons?,” *OIES Paper*, vol. ET, no. 27, 2023.

[12] L. Trevisani, M. Fabbri, and F. Negrini, “Long distance renewable-energy-sources power transmission using hydrogen-cooled MgB2 superconducting line,” *Cryogenics (Guildf)*, vol. 47, no. 2, pp. 113–120, Feb. 2007, doi: 10.1016/j.cryogenics.2006.10.002.

[13] S. Yamada, Y. Hishinuma, T. Uede, K. Schippl, and O. Motojima, “Study on 1 GW class hybrid energy transfer line of hydrogen and electricity,” *J Phys Conf Ser*, vol. 97, p. 012167, Feb. 2008, doi: 10.1088/1742-6596/97/1/012167.

[14] P. M. Grant, “The SuperCable: Dual Delivery of Chemical and Electric Power,” *IEEE Transactions on Appiled Superconductivity*, vol. 15, no. 2, pp. 1810–1813, Jun. 2005, doi: 10.1109/TASC.2005.849298.

[15] Y. Chen *et al.*, “Ultra-low electrical loss superconducting cables for railway transportation: Technical, economic, and environmental analysis,” *J Clean Prod*, vol. 445, p. 141310, Mar. 2024, doi: 10.1016/j.jclepro.2024.141310.

[16] M. Gammelsæter and A. Marian, “SCARLET Project Description.”

[17] L. Savoldi, A. Balbo, C. E. Bruzek, G. Grasso, M. Patti, and M. Tropeano, “Conceptual Design of a SuperConducting Energy Pipeline for LH2 and Power Transmission Over Long Distances,” *IEEE Transactions on Applied Superconductivity*, vol. 34, no. 3, 2024, doi: 10.1109/TASC.2024.3370123.

[18] P. M. Grant, “The SuperCable: Dual Delivery of Chemical and Electric Power,” *IEEE Transactions on Appiled Superconductivity*, vol. 15, no. 2, pp. 1810–1813, Jun. 2005, doi: 10.1109/TASC.2005.849298.

[19] S. Palacios, M. Wehr, Micheal. J. Wolf, M. Noe, and T. Arndt, “Combined Energy Transmission by LH_2 and HTS: Study of a Hybrid Pipeline,” in *16th European Conference on Applied Superconductivity (EUCAS 2023)*, Bologna, 2023. Accessed: Jul. 09, 2025. [Online]. Available: http://dx.doi.org/10.13140/RG.2.2.10355.75046

[20] Ministero dell’Università e della Ricerca, “Portale dei bandi PRIN della Direzione Generale della Ricerca del MUR.” Accessed: Jun. 06, 2025. [Online]. Available: https://prin.mur.gov.it/

[21] M. Bracco *et al.*, “Design of a Submarine 30-km MgB_{2} Cable for the Combined Transfer of 0.3 GW_e and LH_{2} from Offshore Plants to the Ravenna Port,” *IEEE Transactions on Applied Superconductivity*, vol. 35, no. 5, pp. 1–6, Aug. 2025, doi: 10.1109/TASC.2025.3528923.

[22] AGNES, “Eolico Offshore in mare Adriatico.” Accessed: Jun. 28, 2025. [Online]. Available: https://www.agnespower.com/eolico-offshore-adriatico/

[23] Ener2Crowd, “Progetto Agnes Romagna Il primo green energy hub del Mar Mediterraneo.” Accessed: Jun. 28, 2025. [Online]. Available: https://www.ener2crowd.com/it/documenti/progetti/1724-D6A298714CD8452BCE85C6A3DFAF3A2D

[24] P. Laha and B. Chakraborty, “Energy model – A tool for preventing energy dysfunction,” *Renewable and Sustainable Energy Reviews*, vol. 73, pp. 95–114, Jun. 2017, doi: 10.1016/j.rser.2017.01.106.

[25] K. Poncelet, “Long-term energy-system optimization models,” Doctoral Dissertation, Arenberg Doctoral School, 2018. Accessed: Jun. 29, 2025. [Online]. Available: file:///C:/Users/LENOVO/Downloads/thesis_final.pdf

[26] E. Trutnevyte, “Does cost optimization approximate the real-world energy transition?,” *Energy*, vol. 106, pp. 182–193, Jul. 2016, doi: 10.1016/j.energy.2016.03.038.

[27] J. Priesmann, L. Nolting, and A. Praktiknjo, “Are complex energy system models more accurate? An intra-model comparison of power system optimization models,” *Appl Energy*, vol. 255, p. 113783, Dec. 2019, doi: 10.1016/j.apenergy.2019.113783.

[28] M. Nicoli, F. Gracceva, D. Lerede, and L. Savoldi, “Can We Rely on Open-Source Energy System Optimization Models? The TEMOA-Italy Case Study,” *Energies (Basel)*, vol. 15, no. 18, Sep. 2022, doi: 10.3390/en15186505.

[29] S. Fina, B. Heider, and F. Prota, “Unequal Italy: Regional socio-economic disparities in Italy.” [Online]. Available: https://fes.de/unequal-italy

[30] A. Raihan, J. Rahman, T. Tanchangtya, M. Ridwan, and S. Islam, “An overview of the recent development and prospects of renewable energy in Italy,” *Renewable and Sustainable Energy*, 2024, doi: 10.55092/rse20240008.

[31] M. Muratori *et al.*, “Cost of power or power of cost: A U.S. modeling perspective,” *Renewable and Sustainable Energy Reviews*, vol. 77, pp. 861–874, Sep. 2017, doi: 10.1016/j.rser.2017.04.055.

[32] Ministry of Economic Development, Ministry of the Environment and Land and Sea Protection, and Ministry of Infrastructure and Transport, “Integrated National Energy and Climate Plan 2019,” 2019. Accessed: Aug. 19, 2022. [Online]. Available: https://commission.europa.eu/energy-climate-change-environment/implementation-eu-countries/energy-and-climate-governance-and-reporting/national-energy-and-climate-plans_en

[33] Terna S.p.A., “Documento di Descrizione degli Scenari 2024,” 2024. Accessed: Jun. 12, 2025. [Online]. Available: https://download.terna.it/terna/Documento_Descrizione_Scenari_2024_8dce2430d44d101.pdf

[34] R. A. Rodríguez, S. Becker, G. B. Andresen, D. Heide, and M. Greiner, “Transmission needs across a fully renewable European power system,” *Renew Energy*, vol. 63, pp. 467–476, Mar. 2014, doi: 10.1016/j.renene.2013.10.005.

[35] S. Allard, S. Mima, V. Debusschere, T. T. Quoc, P. Criqui, and N. Hadjsaid, “European transmission grid expansion as a flexibility option in a scenario of large scale variable renewable energies integration,” *Energy Econ*, vol. 87, p. 104733, Mar. 2020, doi: 10.1016/j.eneco.2020.104733.

[36] M. Fodstad *et al.*, “Next frontiers in energy system modelling: A review on challenges and the state of the art,” *Renewable and Sustainable Energy Reviews*, vol. 160, p. 112246, May 2022, doi: 10.1016/j.rser.2022.112246.

[37] Z. Guo, L. Ma, P. Liu, I. Jones, and Z. Li, “A multi-regional modelling and optimization approach to China’s power generation and transmission planning,” *Energy*, vol. 116, pp. 1348–1359, Dec. 2016, doi: 10.1016/j.energy.2016.06.035.

[38] TERNA S.p.A., “Download Center | Dati Terna Driving Energy.” Accessed: Jun. 08, 2025. [Online]. Available: https://dati.terna.it/download-center

[39] R. Novo, P. Marocco, G. Giorgi, A. Lanzini, M. Santarelli, and G. Mattiazzo, “Planning the decarbonisation of energy systems: The importance of applying time series clustering to long-term models,” *Energy Conversion and Management: X*, vol. 15, p. 100274, Aug. 2022, doi: 10.1016/j.ecmx.2022.100274.

[40] M. Nicoli, “MATHEP/TEMOA-Italy/docs.” Accessed: Jun. 07, 2025. [Online]. Available: https://github.com/MAHTEP/TEMOA-Italy/tree/main/docs

[41] A. Balbo, G. Colucci, M. Nicoli, and L. Savoldi, “Exploring the Role of Hydrogen to Achieve the Italian Decarbonization Targets Using an Open-Source Energy System Optimization Model,” in *XVI International Conference on Hydrogen Energy and Technologies*, Paris, 2023.

[42] National Agency for New Technologies Energy and Sustainable Economic Development (ENEA), “The TIMES-Italy Energy Model Structure and Data 2010 Version,” Rome, 2011. Accessed: Sep. 02, 2022. [Online]. Available: https://biblioteca.bologna.enea.it/RT/2011/2011_9_ENEA.pdf

[43] G. Colucci, D. Lerede, M. Nicoli, and L. Savoldi, “A dynamic accounting method for CO2 emissions to assess the penetration of low-carbon fuels: application to the TEMOA-Italy energy system optimization model,” *Appl Energy*, vol. 352, no. 121951, Dec. 2023, doi: 10.1016/j.apenergy.2023.121951.

[44] G. Colucci, D. Lerede, M. Nicoli, and L. Savoldi, “Dynamic Accounting for End-Use CO2 Emissions From Low-Carbon Fuels in Energy System Optimization Models,” *Energy Proceedings*, vol. 29, 2022, doi: 10.46855/energy-proceedings-10294.

[45] Sofia. Simoes *et al.*, “The JRC-EU-TIMES model - Assessing the long-term role of the SET Plan Energy technologies,” p. 376, 2013, doi: 10.2790/97799.

[46] National Renewable Energy Laboratory (NREL), “2022 Annual Technology Baseline (ATB) Cost and Performance Data for Electricity Generation Technologies,” Golden, CO: National Renewable Energy Laboratory. Accessed: Jul. 06, 2023. [Online]. Available: https://atb.nrel.gov/electricity/2022/about

[47] National Renewable Energy Laboratory (NREL), “Useful Life | Energy Analysis | NREL.” Accessed: Jul. 06, 2023. [Online]. Available: https://www.nrel.gov/analysis/tech-footprint.html

[48] M. Nicoli, V. A. D. Faria, A. R. de Queiroz, and L. Savoldi, “Modeling energy storage in long-term capacity expansion energy planning: an analysis of the Italian system,” *J Energy Storage*, vol. 101, p. 113814, Nov. 2024, doi: 10.1016/j.est.2024.113814.

[49] Terna, “‘Italy-France’ Electrical Connection.” Accessed: Nov. 01, 2023. [Online]. Available: https://www.terna.it/en/projects/projects-common-interest/italy-france-electrical-interconnection

[50] Terna, “Cross-border Capacity.” Accessed: Nov. 01, 2023. [Online]. Available: https://www.terna.it/en/electric-system/electricity-market/capacity-interconnection-abroad

[51] Joint Research Center (JRC), “European Meteorological derived High Resolution RES generation time series for present and future scenarios (EMHIRES),” 2021. Accessed: Jul. 12, 2023. [Online]. Available: https://data.jrc.ec.europa.eu/collection/id-0055

[52] Eurostat, “NUTS - Nomenclature of territorial units for statistics.” Accessed: Jul. 12, 2023. [Online]. Available: https://ec.europa.eu/eurostat/web/nuts/background

[53] Terna, “Electric System.” Accessed: Jul. 10, 2023. [Online]. Available: https://www.terna.it/en/electric-system

[54] il POST, “Il complicato rapporto tra la Sardegna e i parchi eolici,” Jul. 31, 2024. Accessed: Jun. 29, 2025. [Online]. Available: https://www.ilpost.it/2024/07/31/opposizione-parchi-eolici-sardegna/

[55] P. Ruiz *et al.*, “ENSPRESO - an open, EU-28 wide, transparent and coherent database of wind, solar and biomass energy potentials,” *Energy Strategy Reviews*, vol. 26, p. 100379, Nov. 2019, doi: 10.1016/J.ESR.2019.100379.

[56] Ministry of Economic Development, “Long term Italian strategy for greenhouse gas emission reduction,” 2021. Accessed: Jun. 21, 2022. [Online]. Available: https://ec.europa.eu/clima/sites/lts/lts_it_it.pdf

[57] European Council, “Fit for 55 - The EU’s plan for a green transition.” Accessed: Jan. 29, 2023. [Online]. Available: https://www.consilium.europa.eu/en/policies/green-deal/fit-for-55-the-eu-plan-for-a-green-transition/

[58] TERNA S.p.A., “Electric system | Terna Driving Energy.” Accessed: Jun. 10, 2025. [Online]. Available: https://www.terna.it/en/electric-system/transparency-report/total-load

[59] A. Alberini, G. Prettico, C. Shen, and J. Torriti, “Hot weather and residential hourly electricity demand in Italy,” *Energy*, vol. 177, pp. 44–56, Jun. 2019, doi: 10.1016/j.energy.2019.04.051.

[60] Istat, “Popolazione residente per sesso, età e stato civile al 1° gennaio 2022.” Accessed: Jun. 11, 2025. [Online]. Available: https://demo.istat.it/app/?l=it&a=2022&i=POS

[61] Istat, “Prodotto interno lordo lato produzione - edizioni gennaio 2020 - dicembre 2023.” Accessed: Jun. 11, 2025. [Online]. Available: https://esploradati.istat.it/databrowser/#/it/dw/categories/IT1,DATAWAREHOUSE,1.0/ACC_B19/ACC_TERRIT_B19/IT1,6_498_DF_DCCN_PILT_B19_1,1.0

[62] M. Nicoli, “An energy planning perspective about the multi-sectorial synergies and implications of the energy transition,” PhD Thesis, Politecnico di Torino, Turin, 2025. Accessed: Jul. 07, 2025. [Online]. Available: https://iris.polito.it/handle/11583/3001281

[63] G. Colucci, D. Lerede, M. Nicoli, and L. Savoldi, “A dynamic accounting method for CO2 emissions to assess the penetration of low-carbon fuels: application to the TEMOA-Italy energy system optimization model,” *Accepted for Publication in Applied Energy*, 2023.

[64] Eurostat, “Energy balances - Energy - Eurostat.” Accessed: Aug. 19, 2022. [Online]. Available: https://ec.europa.eu/eurostat/web/energy/data/energy-balances

[65] M. Gandiglio and P. Marocco, “Mapping Hydrogen Initiatives in Italy: An Overview of Funding and Projects,” *Energies (Basel)*, vol. 17, no. 11, p. 2614, May 2024, doi: 10.3390/en17112614.

[66] MAHTEP Group, “MAHTEP/TEMOA-Italy,” GitHub. Accessed: May 11, 2022. [Online]. Available: https://github.com/MAHTEP/TEMOA-Italy

[67] S. Gago Da Camara Simoes *et al.*, “The JRC-EU-TIMES model - Assessing the long-term role of the SET Plan Energy technologies,” *Publications Office of the European Union*, 2013, doi: 10.2790/97799.

[68] International Energy Agency (IEA), “The Future of Hydrogen,” 2019. Accessed: Jun. 12, 2025. [Online]. Available: https://iea.blob.core.windows.net/assets/9e3a3493-b9a6-4b7d-b499-7ca48e357561/The_Future_of_Hydrogen.pdf

[69] IRENA, “Green hydrogen cost reduction scaling up electrolysers to meet the 1.5°C climate goal,” 2020. Accessed: Jun. 12, 2025. [Online]. Available: https://www.irena.org/-/media/Files/IRENA/Agency/Publication/2020/Dec/IRENA_Green_hydrogen_cost_2020.pdf?rev=4ce868aa69b54674a789f990e85a3f00

[70] Z. Cheng, “Global Hydrogen Demand: Analysis and Integration into the Market Model,” Technical University of Munich, Munich, 2024. Accessed: Jun. 13, 2025. [Online]. Available: https://www.ffe.de/wp-content/uploads/2024/11/Masterarbeit-Cheng-Zhibin.pdf

[71] J. Cader, R. Koneczna, and P. Olczak, “The Impact of Economic, Energy, and Environmental Factors on the Development of the Hydrogen Economy,” *Energies (Basel)*, vol. 14, no. 16, p. 4811, Aug. 2021, doi: 10.3390/en14164811.

[72] G. Colucci, D. Lerede, M. Nicoli, and L. Savoldi, “A dynamic accounting method for CO2 emissions to assess the penetration of low-carbon fuels: application to the TEMOA-Italy energy system optimization model,” *Appl Energy*, vol. 352, p. 121951, Dec. 2023, doi: 10.1016/j.apenergy.2023.121951.

[73] World Bank, “World Bank Commodities Price Forecast (nominal US dollars)-2022,” 2022. Accessed: Aug. 04, 2023. [Online]. Available: https://thedocs.worldbank.org/en/doc/d8730a829c869c7aeaba547eb72d6b3f-0350012022/related/CMO-October-2022-forecasts.pdf

[74] M. Nicoli *et al.*, “Enabling Coherence Between Energy Policies and SDGs Through Open Energy Models: The TEMOA-Italy Example,” in *Aligning the Energy Transition with the Sustainable Development Goals: Key Insights from Energy System Modelling*, M. Labriet, K. Espegren, G. Giannakidis, and B. O’Gallachoir, Eds., Springer, 2024, pp. 97–118. doi: 10.1007/978-3-031-58897-6_5.

[75] United States Environmental Protection Agency, “Basic Information of Air Emissions Factors and Quantification.” Accessed: Jun. 27, 2025. [Online]. Available: https://www.epa.gov/air-emissions-factors-and-quantification/basic-information-air-emissions-factors-and-quantification

[76] A. De Vita and P. Capros, “EU reference scenario 2020 – Energy, transport and GHG emissions – Trends to 2050,” 2021. Accessed: Jun. 25, 2025. [Online]. Available: https://op.europa.eu/en/publication-detail/-/publication/96c2ca82-e85e-11eb-93a8-01aa75ed71a1/language-en

[77] Terna S.p.A., *Allegato A24 al Codice di Rete | Individuazione zone della rete rilevante*. Italy, 2020. Accessed: Jun. 14, 2025. [Online]. Available: https://www.terna.it/it/sistema-elettrico/pubblicazioni/news-operatori/dettaglio/Suddivisione-in-zone-di-mercato-della-Rete-di-Trasmissione-Nazionale-valida-a-partire-dal-1%C2%B0-gennaio-2021

[78] Terna S.p.A., “Stato del Sistema Elettrico 2023,” 2023. Accessed: Jun. 14, 2025. [Online]. Available: https://download.terna.it/terna/Terna_Piano_Sviluppo_2023_Stato_Sistema_Elettrico_8db254887149b77.pdf

[79] K. Vaillancourt, G. Simbolotti, and G. Tosato, “Electricity Transmission and Distribution,” 2014, *IEA Energy Technology Systems Analysis Program (ESTAP)*. Accessed: Jun. 14, 2025. [Online]. Available: https://iea-etsap.org/E-TechDS/PDF/E12_el-t&d_KV_Apr2014_GSOK.pdf

[80] D. L’Erede, “PyPSA | technology-data Public.” Accessed: Jun. 14, 2025. [Online]. Available: https://github.com/PyPSA/technology-data/blob/master/inputs/manual_input.csv

[81] S. Hagspiel, C. Jägemann, D. Lindenberger, T. Brown, S. Cherevatskiy, and E. Tröster, “Cost-optimal power system extension under flow-based market coupling,” *Energy*, vol. 66, pp. 654–666, Mar. 2014, doi: 10.1016/j.energy.2014.01.025.

[82] P. Härtel, T. K. Vrana, T. Hennig, M. von Bonin, E. J. Wiggelinkhuizen, and F. D. J. Nieuwenhout, “Review of investment model cost parameters for VSC HVDC transmission infrastructure,” *Electric Power Systems Research*, vol. 151, pp. 419–431, Oct. 2017, doi: 10.1016/j.epsr.2017.06.008.

[83] T. Borsboom-Hanson, S. R. Patlolla, O. E. Herrera, and W. Mérida, “Point-to-point transportation: The economics of hydrogen export,” *Int J Hydrogen Energy*, vol. 47, no. 74, pp. 31541–31550, Aug. 2022, doi: 10.1016/j.ijhydene.2022.07.093.

[84] F. Ganda and G. Maronati, “Economic Data and Modeling Support for the Two Regional Case Studies: Nuclear-Renewable Hybrid Energy Systems: Analysis of Technical & Economic Issues,” Argonne, IL (United States), Aug. 2018. doi: 10.2172/1483989.

[85] The Danish Energy Agency, “Technology Data for Transport of Energy.” Accessed: Jun. 14, 2025. [Online]. Available: https://ens.dk/en/analyses-and-statistics/technology-data-transport-energy

[86] T. Galimova, M. Fasihi, D. Bogdanov, and C. Breyer, “Impact of international transportation chains on cost of green e-hydrogen: Global cost of hydrogen and consequences for Germany

and Finland," *Appl Energy*, vol. 347, p. 121369, Oct. 2023, doi: 10.1016/j.apenergy.2023.121369.

[87] S. ZS. Al Ghafri *et al.*, "Hydrogen liquefaction: a review of the fundamental physics, engineering practice and future opportunities," *Energy Environ Sci*, vol. 15, no. 7, pp. 2690–2731, 2022, doi: 10.1039/D2EE00099G.

[88] European Commission, *Communication from the Commission | The European Green Deal*. 2019. Accessed: Jun. 17, 2025. [Online]. Available: https://eur-lex.europa.eu/legal-content/EN/LSU/?uri=COM:2019:640:FIN

[89] Ministero dell'Ambiente e della Tutela del Territorio e del Mare, Ministero dello Sviluppo Economico, Ministero delle Infrastrutture e dei Trasporti, and A. e F. Ministero delle Politiche agricole, *Strategia Italiana di Lungo Termine sulla riduzione delle emissioni dei gas a effetto serra*. Italy, 2021. Accessed: Jun. 17, 2025. [Online]. Available: https://www.mase.gov.it/portale/documents/d/guest/lts_gennaio_2021-pdf

[90] H. Su, N. Zhou, Q. Wu, Z. Bi, and Y. Wang, "Investigating price fluctuations in copper futures: Based on EEMD and Markov-switching VAR model," *Resources Policy*, vol. 82, p. 103518, May 2023, doi: 10.1016/j.resourpol.2023.103518.